Graduate School ETD Form 9
(Revised 12/07)

PURDUE UNIVERSITY
GRADUATE SCHOOL
Thesis/Dissertation Acceptance

This is to certify that the thesis/dissertation prepared

By Yao Zhai

Entitled Design of Switching Strategy for Adaptive Cruise Control Under String Stability Constraints

For the degree of Master of Science in Electrical and Computer Engineering

Is approved by the final examining committee:

Yaobin Chen
Chair

Glenn R. Widmann

Lingxi Li

To the best of my knowledge and as understood by the student in the *Research Integrity and Copyright Disclaimer (Graduate School Form 20)*, this thesis/dissertation adheres to the provisions of Purdue University's "Policy on Integrity in Research" and the use of copyrighted material.

Approved by Major Professor(s): Yaobin Chen

Approved by: Yaobin Chen 12/06/2010
Head of the Graduate Program Date

Graduate School Form 20
(Revised 9/10)

PURDUE UNIVERSITY
GRADUATE SCHOOL

Research Integrity and Copyright Disclaimer

Title of Thesis/Dissertation:

Design of Switching Strategy for Adaptive Cruise Control Under String Stability Constraints

For the degree of Master of Science in Electrical and Computer Engineering

I certify that in the preparation of this thesis, I have observed the provisions of *Purdue University Executive Memorandum No. C-22,* September 6, 1991, *Policy on Integrity in Research.**

Further, I certify that this work is free of plagiarism and all materials appearing in this thesis/dissertation have been properly quoted and attributed.

I certify that all copyrighted material incorporated into this thesis/dissertation is in compliance with the United States' copyright law and that I have received written permission from the copyright owners for my use of their work, which is beyond the scope of the law. I agree to indemnify and save harmless Purdue University from any and all claims that may be asserted or that may arise from any copyright violation.

Yao Zhai

Printed Name and Signature of Candidate

12/06/2010

Date (month/day/year)

*Located at http://www.purdue.edu/policies/pages/teach_res_outreach/c_22.html

DESIGN OF SWITCHING STRATEGY FOR ADAPTIVE CRUISE CONTROL UNDER STRING STABILITY CONSTRAINTS

A Thesis
Submitted to the Faculty
of
Purdue University
by
Yao Zhai

In Partial Fulfillment of the
Requirements for the Degree
of
Master of Science in Electrical and Computer Engineering

December 2010
Purdue University
Indianapolis, Indiana

ACKNOWLEDGEMENTS

I would like to thank my advisor, Professor Yaobin Chen, for his guidance, encouragement, long-term support, and patience during the entire process of my research and thesis work, without which I cannot even imagine how I could get where I am today. He is not only being helpful in my research work, but also a mentor in every aspect of my life. I hereby give my full gratitude to Professor Yaobin Chen.

I would also like to thank Dr. Glenn R. Widmann of Delphi Electronics and Safety for his insightful advice on my thesis research, which inspired me to revise the whole idea of headway control algorithm. A major part of this thesis has been derived according to his suggestions, by which I have been greatly encouraged.

I would like to express my great appreciation to Professor Lingxi Li, for his consistent support to each and every level of my research. He has been giving me tremendous help and useful suggestions. Whenever I have trouble, I know I can always go to him for help. He also gave me suggestions about how to write a thesis, which I have profited from.

Finally, I would also like to thank Ms. Valerie Lim Diemer for her help on formatting this thesis and guidance throughout my graduate study. I am also grateful for my friends Dr. Yiqiang Li, from China Agricultural University, Hong Fu from Tsinghua University, Dr. Xiao Lin from Zhejiang University and lab mate Jie Xue, for their helpful comments and suggestions which help me improve my research and thesis.

TABLE OF CONTENTS

Page

LIST OF FIGURES

Figure Page

ABSTRACT

Zhai, Yao. M.S.E.C.E., Purdue University, December, 2010. Design of Switching Strategy for Adaptive Cruise Control under String Stability Constraints. Major Professor: Yaobin Chen.

An Adaptive Cruise Control (ACC) system is a driver assistance system that assists a driver to improve driving safety and driving comfort. The design of ACC controller often involves the design of a switching logic that decides where and when to switch between the two modes in order to ameliorate driving comfort, mitigate the chance of a potential collision with the preceding vehicle while reduce long-distance driving load from the driver.

In this thesis, a new strategy for designing ACC controller is proposed. The proposed control strategy utilizes Range vs. Range-rate chart to illustrate the relationship between headway distance and velocity difference, and then find out a constant deceleration trajectory on the chart, which the following vehicle is controlled to follow. This control strategy has a shorter elapsed time than existing ones while still maintaining a relatively safe distance during transient process. String stability issue has been addressed by many researchers after the adaptive cruise control (ACC) concept was developed. The main problem is when many vehicles with ACC controller forming a vehicle platoon end to end, how the control algorithm is designed to ensure that the spacing error, which is the deviation of the actual range from the desired headway distance, would not amplify as the number of following vehicles increases downstream along the platoon. In this thesis, string stability issues have been taken into consideration

and constraints of parameters of an ACC controller are derived to mitigate steady state error propagation.

1. INTRODUCTION

An Adaptive Cruise Control (ACC) system is a driver assistance system that assists driver to improve driving safety and driving comfort. Adaptive cruise control is similar to conventional cruise control already available in most passenger cars in that, it maintains the vehicle's pre-set speed in the absence of preceding vehicles. However, unlike conventional cruise control, an ACC system can automatically adjust speed in order to maintain a proper spacing between the slower preceding vehicle and the subject vehicle.

In order to achieve such functionality, each ACC equipped vehicle has radar and/or other sensor(s) such as lidar that measures the distance to the preceding vehicle and calculates the relative velocity of the preceding vehicle according to its own speed [1, 2].

The ACC system is a longitudinal control strategy comprised of two distinct operational control modes, speed control mode and headway control mode. During normal driving when no preceding vehicle is present, ACC controller operates in the speed control mode and functions as a conventional cruise controller that maintains the speed of the subject vehicle to a driver pre-set speed. Once a preceding vehicle is detected, either because of a cut-in or encounters of slower moving vehicle ahead, the ACC system switches from cruise control mode to headway control mode. In headway control mode, a desired safety distance from the preceding vehicle to the subject vehicle is maintained, in order to mitigate possibilities of any collision, and ameliorate driving comfort at the same time.

As part of the Automated Highway Systems (AHS) program conducted during the late 90s, adaptive cruise control systems were paid a lot of attention to and intense research and development were carried out by several research groups, most notably by the California PATH program at the University of California, Berkeley [3]. The objective of the AHS program was to dramatically improve the traffic capacity on a highway by enabling vehicles to run together in a tightly spaced platoon. Only adequately equipped vehicles are allowed to drive on a specially designed highway segment, while manually driven vehicles are not [4].

Since then, much research has been conducted mainly in three categories: autonomous control, semi-autonomous control and centralized control of intelligent vehicles [4-6]. Autonomous control of a vehicle refers to methods that solely depend on information collected by sensors located on the subject vehicle, while semi-autonomous control, in comparison, refers to control methods that also depend on information sent back and forth among vehicles, which requires vehicle-to-vehicle communication systems and vehicle networks. The last category, centralized control, requires not only vehicle-to-vehicle communication systems but also vehicle to infrastructure communication systems as well. The idea is that a centralized supervisory controller outside the platoon of intelligent vehicles is going to be in charge of each of the vehicles in the platoon, such as to adjust the velocity of each vehicle and the spacing range between consecutive vehicles [6].

While the last two categories (semi-autonomous and centralized control) are not practical traffic control implementation realizations in the near future, an autonomous control strategy using an ACC system, is however a very attractive feature consideration right now and is already available in the market [7]. Radar-based ACC systems have been in series production since 1999.

With the increase market availability of ACC systems in the vehicle fleet, then another question arises with the implementation of such system. Envision that a multitude

of ACC-equipped vehicles operating in a platoon traffic scenario on a highway, all of which have the ACC system engaged. The objective of this thesis is to investigate the string stability issues related to the platoon string as a whole and the design of an ACC control strategy that addresses the platoon stability. Several researchers have already paid much attention to this issue in their previous works [3, 6, 8, 9].

The primary idea of developing ACC systems and furthermore, Automated Highway Systems described above has been fueled by a number of motivations, including the purpose to better improve driver comfort and driving safety. An ACC system not only takes control of the vehicle when it's engaged, it also serves as a warning system that reminds the driver of appearance of any potential danger. ACC systems and other automated systems in general are assumed to contribute to improvement of safety on the highway. Statistics show that over 90% of accidents are caused by human errors [10], while only a relatively small percentage of accidents are the result of vehicle function failure or due to environmental conditions such as icy road. The ACC system and other Automated Highway technologies alleviate driver burden and provide driver assistance, it's expected that the use of such technologies will noticeably lead to reduction of accidents.

This thesis work is focused on design a new ACC control strategy that takes into consideration the string stability issues in platoon scenario. Based on Rate vs. Range-rate chart, a new switching logic for designing ACC controllers systematically with shorter transient time has been proposed in this Thesis. Simulation based on the proposed design steps has been carried out and results are presented. String stability issues have been taken into consideration and constraints for controller parameters were derived in order to mitigate steady state error propagation. Two different definitions of desired headway distance have been discussed and string stability constraints under both definitions have been considered and derived.

The remainder of this thesis is organized as following. Chapter 2 describes a longitudinal model of vehicle dynamics used in this thesis. Using Matlab/Simulink platform, all the simulation results are based on such model of vehicle dynamics. Chapter 3 presents a generalized method of developing an Adaptive Cruise Controller along with its quantitative analysis of performance. Chapter 4 elaborates in details the issue of string stability mentioned above. Simulation results are also presented and discussed in Chapter 4. And Chapter 5 concludes the thesis and provides recommendations for future work.

2. MODEL OF VEHICLE DYNAMICS

The control of longitudinal motion has been examined by many researchers and engineers. In order to facilitate the development of a longitudinal controller for ACC system that addresses the platoon stability control issue, a realistic model representing the vehicle's longitudinal dynamics is necessary. Simulation techniques will be utilized to identify system deficiencies and alter control algorithms to improve and verify performance.

This chapter presents a dynamic model for the longitudinal control of vehicle motion, which includes two major parts, vehicle dynamics and powertrain dynamics. Longitudinal tire forces, aerodynamic drag forces, rolling resistance forces and gravitational forces will be described in the discussion about the vehicle dynamics. The engine model, the torque converter model, the transmission model and the wheel model will be included in the discussion about powertrain dynamics.

2.1. Longitudinal Vehicle Model

Imagine a vehicle running on an inclined road as shown in Figure 2.1 [11]. $G = mg$ is the gravity of the vehicle, where m is the vehicle mass and g is the gravity acceleration; α is the incline angle of the road; h_g is the height of the vehicle's Center of Gravity(CG); T_{f1} and T_{f2} are torques applied to the front and rear wheels; F_{X1} and F_{X2} are longitudinal forces on the vehicle at the front and rear wheel ground contact points, respectively; F_{Zw1} and F_{Zw2} are vertical load forces on the vehicle at the front and rear ground contact points, respectively; u_d is the longitudinal vehicle velocity and $\frac{du}{dt}$ is the

longitudinal acceleration of the vehicle, where a and b are the distances between CG and the front and rear axles, respectively.

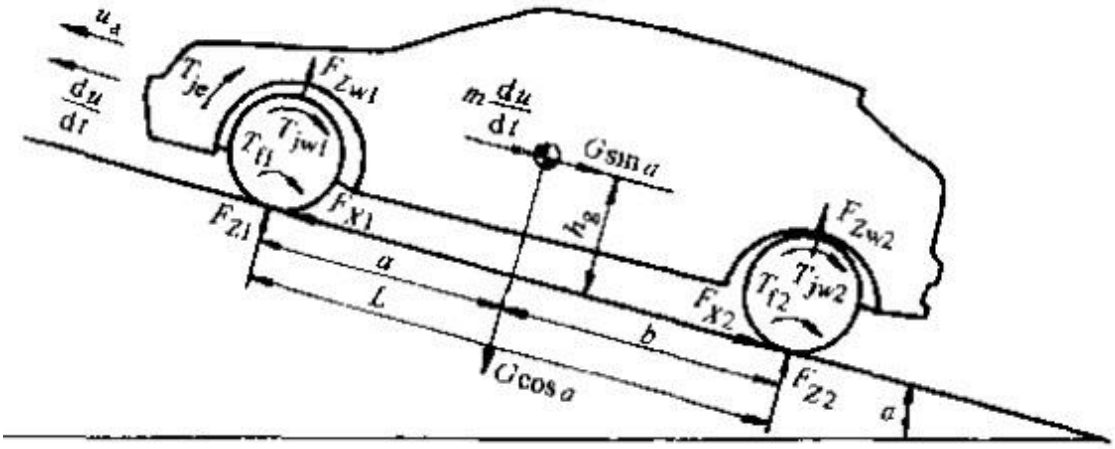

Figure 2.1 Vehicle Dynamics and Motion

The external longitudinal forces acting on the vehicle include longitudinal tire forces, gravitational forces, aerodynamic drag forces and rolling resistance forces. The vehicle motion is determined by the net effect of all these external forces and torques applied on it. The following equations describe all the relationships among these external forces [11, 12].

$$m\frac{du}{dt} = F_X + F_d - mg \cdot \sin\alpha \tag{2.1}$$

$$F_X = F_{X1} + F_{X2} \tag{2.2}$$

$$F_d = -0.5C_d\rho A u_d^2 \cdot sgn(u_d) \tag{2.3}$$

where C_d is the air drag coefficient, A is the frontal area and ρ is the air density.

From vertical perspective, zero vertical acceleration and zero pitch torque require

$$F_{Zw1} = \frac{+h_g(F_d - mg\sin\alpha - m\dot{u}_d) + b \cdot mg\cos\alpha}{a+b} \tag{2.4}$$

$$F_{Zw2} = \frac{+h_g(F_d - mg\,sin\,\alpha - m\dot{u}_d) + a \cdot mg\,cos\,\alpha}{a + b} \tag{2.5}$$

where

$$F_{Zw1} + F_{Zw2} = mg\,cos\,\alpha \tag{2.6}$$

2.2. Engine Model

If the intake manifold filling dynamics are ignored, a first order engine model can be used to represent engine dynamics. It's still valid to use such engine model for some longitudinal vehicle control applications if the bandwidth of the control system to be designed is low [13].

In the case where a first order model is used for simulation, the engine dynamics consist of just one state ω_e, the rotational velocity of an engine and is given by

$$I_e\dot{\omega}_e = T_{net} - T_{load} \tag{2.7}$$

where I_e is the engine inertia, T_{load} is the load torque and $T_{net}(\alpha, \omega_e)$ is the net torque after losses, and can be obtained from an engine map. $T_{net}(\alpha, \omega_e)$ is provided as a steady state function of the engine rotational velocity ω_e and the throttle angle α as inputs.

Figure 2.2 represents a typical engine map with engine rotational velocity ω_e and the throttle angle α as inputs, the net torque after losses $T_{net}(\alpha, \omega_e)$ as output [12]. It's clear that $T_{net}(\alpha, \omega_e)$ increases with throttle angle nonlinearly but monotonically. For each throttle, $T_{net}(\alpha, \omega_e)$ initially increases with rotational engine velocity ω_e, reaches a maximum and then decreases.

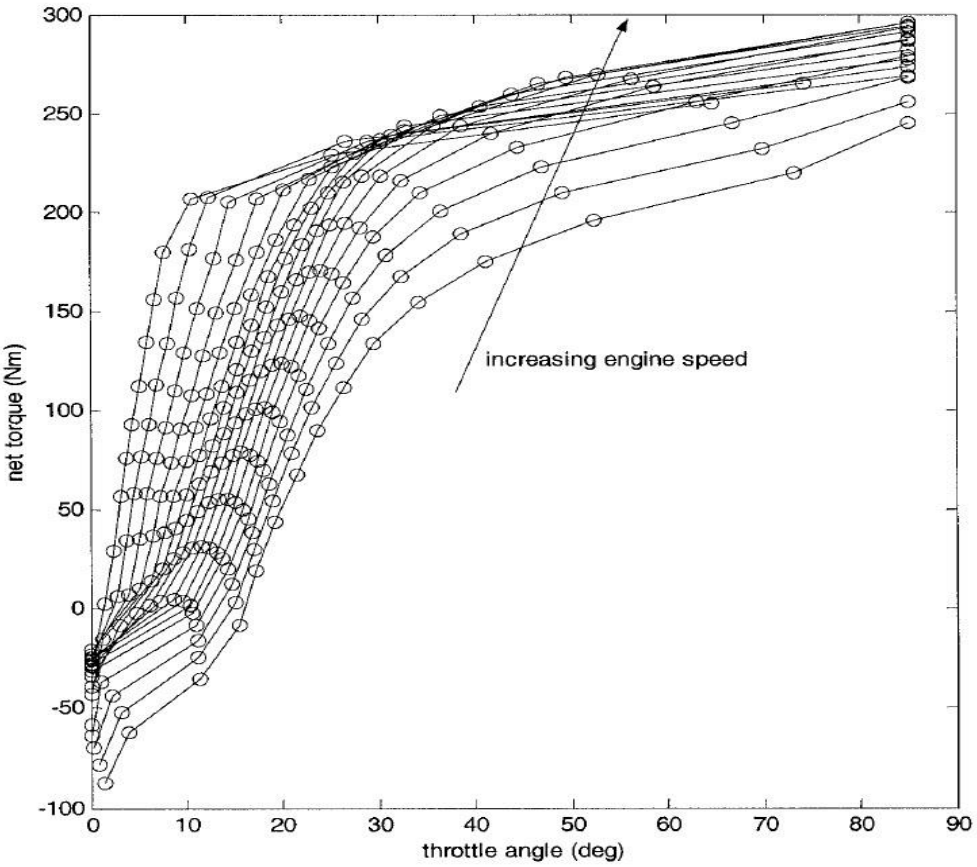

Figure 2.2 First Order Engine Map

Thus for each throttle angle, there is an engine speed ω_e at which maximum torque is achieved, because throttle angle α relates to the pressure in the intake manifold of an engine, as seen in Figure 2.3.

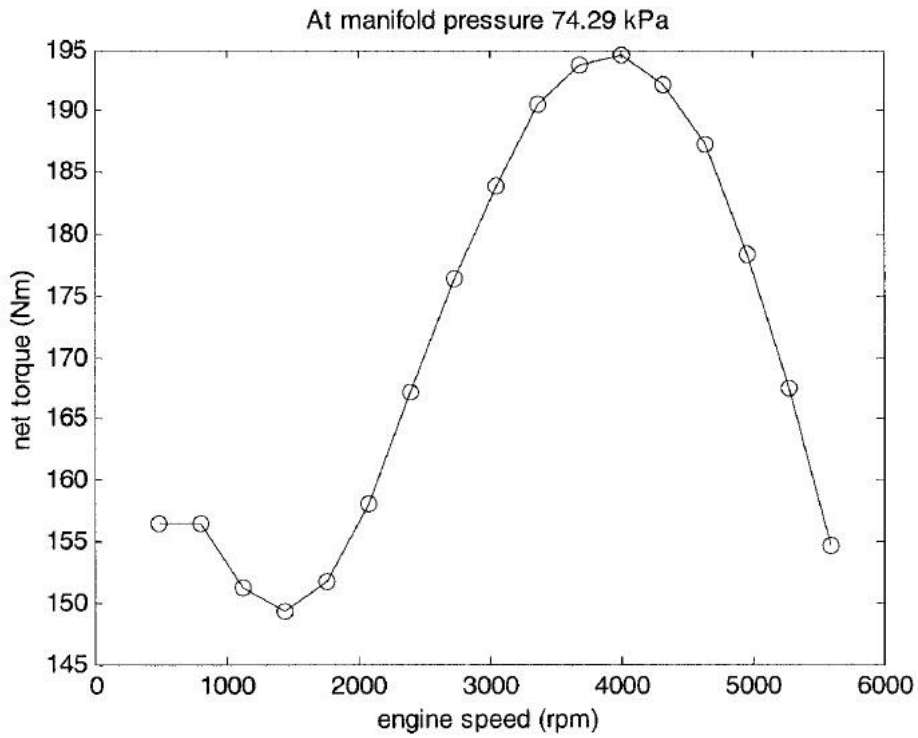

Figure 2.3 $T_{net}(\alpha, \omega_e)$ as a Function of ω_e for Certain Throttle Angle α

The engine model used in this thesis uses a programmed relationship between torque and speed, modulated by the throttle signal, according to the engine characteristics described above.

An engine torque demand function $g(\omega_e)$ is built into the engine dynamic block, which provides the maximum torque available for a given engine speed ω_e. The throttle input α specifies the actual engine torque delivered as a fraction of the maximum torque possible in a steady state at a fixed engine revolution. The actual torque delivered from the engine is modulated as $T_{net} = \alpha \cdot g(\omega_e)$. Then the actual engine drive shaft speed ω_e is fed back to the engine input.

The demand function $g(\omega_e)$ is defined in terms of the steady-state engine power $P(\omega_e)$. The range of the engine speed is limited from 0 to ω_{emax}, and the maximum engine power P_{max} defines ω_{emax} such that $P_{max} = P(\omega_{emax})$. Then define $\omega =$

ω_e/ω_{emax} and $P(\omega_e) = P_{max} \cdot p(\omega)$. Since power is the product of torque and angular velocity, the torque demand function is thus

$$g(\omega_e) = \left(\frac{P_{max}}{\omega_{emax}}\right) \cdot \left[\frac{p(\omega)}{\omega}\right] \tag{2.8}$$

Then from Figure 2.2, by using polynomial fitting, a polynomial form of $p(\omega)$ can be derived as

$$p(\omega) = p1 \cdot \omega + p2 \cdot \omega^2 - p3 \cdot \omega^3 \tag{2.9}$$

where $p1 + p2 - p3 = 1$ and $p1 + 2p2 - p3 = 0$. A typical engine power demand function can be shown as Figure 2.4 [14].

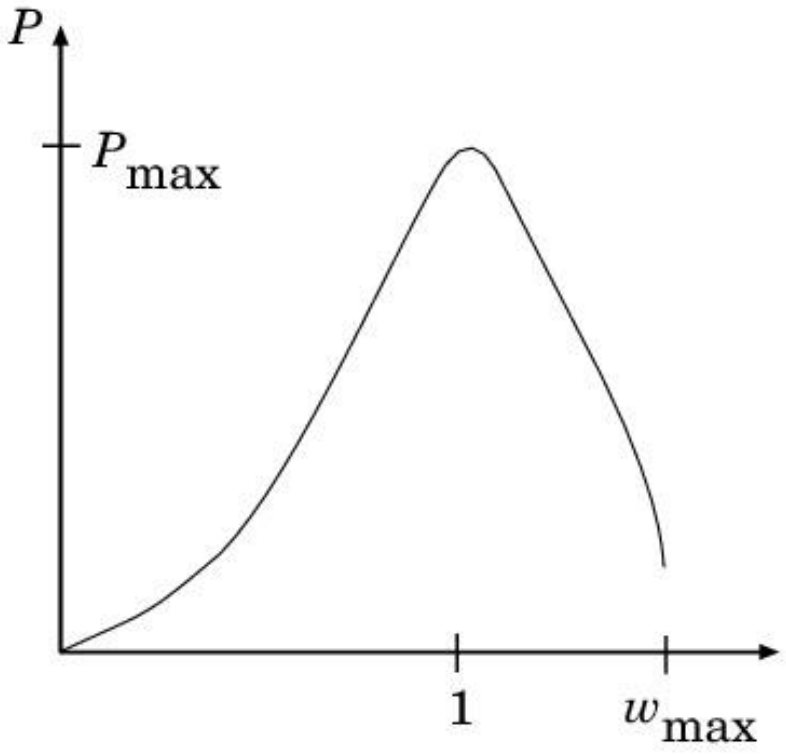

Figure 2.4 A Typical Engine Power Demand Function

2.3. Drivetrain Dynamic

Through powertrain dynamic the power generated by engine flows from the engine to the wheels, and load flows backwards from wheels to the engine shaft [15], shown as in Figure 2.5.

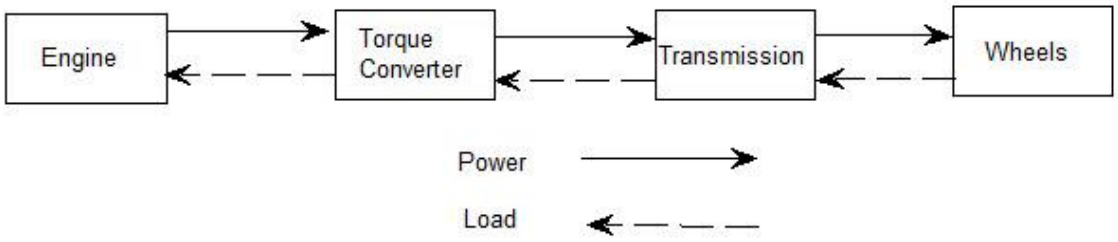

Figure 2.5 Power and Load Flow in a Vehicle Drivetrain

2.3.1. Torque Converter

Torque converter is the equipment that couples torque from engine side to the transmission side and couples load backwards. It consists of two major components, a pump on the engine side and a turbine on the transmission side. The fins of the pump are attached to the flywheel of the engine and therefore turn at the same speed as the engine. The turbine is connected to the transmission and causes the transmission to spin at the same speed as the turbine, and then basically this mechanism moves the wheels after torque is passed through the gear box of the transmission [12].

Torque converter has three operational modes, stall mode, acceleration mode and coupling mode. During stall mode when the engine shaft is transferring power to the pump but the turbine cannot rotate due to constant braking, the torque converter can produce maximum torque multiplication (called stall ratio in this case) if sufficient input power is applied. When the load is accelerating but there still is a relatively large difference between pump and turbine speed, the torque converter works in acceleration mode. In this case, the amount of multiplication will depend upon the actual difference speed of the pump and the turbine.

The coupling mode of the torque converter is the main working mode. In this mode, the turbine has reached over 90% of the speed of the pump. Torque multiplication has basically ceased and the torque converter is working as a plain fluid coupling. Usually in this mode, a lock-up clutch is applied to improve fuel efficiency.

In the simulation model on which this thesis is based, an assumption is made such that the torque converter is always working in the coupling mode and the loss caused by the torque converter is neglected.

2.3.2. Transmission Model

Transmission, a.k.a. gearbox, provides speed and torque from the engine through connection with the turbine in torque converter. Often, a transmission will have multiple gear ratios, with the ability to switch between them as speed varies [16].

In the simulation used by this thesis, two differential blocks are used to represent differential gear that couples rotational motion about the longitudinal axis to rotational motion of the tow lateral axes. In terms of the driving gear ratio g_D, the longitudinal motion is related to the sum of the lateral motions,

$$\omega_B = 0.5 \cdot g_D \cdot (\omega_{F1} + \omega_{F2}) \tag{2.10}$$

where ω_{F1} and ω_{F2} are the speeds of the front wheels and the sum of the motion is the transformed longitudinal motion, as long as the longitudinal axis is connected.

The torques along the lateral axes, T_{F1} and T_{F2} are constrained to the longitudinal torque input, in a superposition way,

$$\omega_B T_B = \omega_{F1} T_{F1} + \omega_{F2} T_{F2} \tag{2.11}$$

Combining Equation 2.10 and Equation 2.11, we have

$$g_D T_B = \frac{2(\omega_{F1} T_{F1} + \omega_{F2} T_{F2})}{\omega_{F1} + \omega_{F2}} \tag{2.12}$$

where g_D is the transmission gear ratio. Equation 2.12 is the transmission model used in the simulation [17].

2.3.3. Wheel Model

The tire is a flexible body what contacts the road surface and gives the subject on it the force needed to move forward or backward. When a torque is applied to the wheel axle, the tire deforms, pushes the ground and delivers a reverse force back from the ground to the wheel, and then pushes the wheel forward or backward.

Longitudinal forces F_{Zw1} and F_{Zw2} in Equation 2.4 and Equation 2.5 are friction forces from the ground that act on the tires, which depend on three factors, the slip ratio, the normal load on each tire and the friction coefficient of the tire-road interface [18].

A longitudinal slip of a tire is defined as the difference between the actual longitudinal velocity at the axle of the wheel, u_d in Figure 2.1, and the equivalent rotational velocity $r_{eff}\omega_w$ of the tire, where r_{eff} is the effective tire radius and ω_w is the rotational speed of the wheel. In other words, longitudinal slip is equal to $r_{eff}\omega_w - u_d$.

Longitudinal slip ratio is defined differently during different situations.

During braking:

$$\sigma_x = \frac{r_{eff}\omega_w - u_d}{u_d} \tag{2.13}$$

During acceleration:

$$\sigma_x = \frac{r_{eff}\omega_w - u_d}{r_{eff}\omega_w} \tag{2.14}$$

From experimental data, Figure 2.6 shows why and how slip ratio affects longitudinal tire forces. It is clear that in the case where longitudinal slip is small, the longitudinal tire force is approximately proportional to the slip ratio [18].

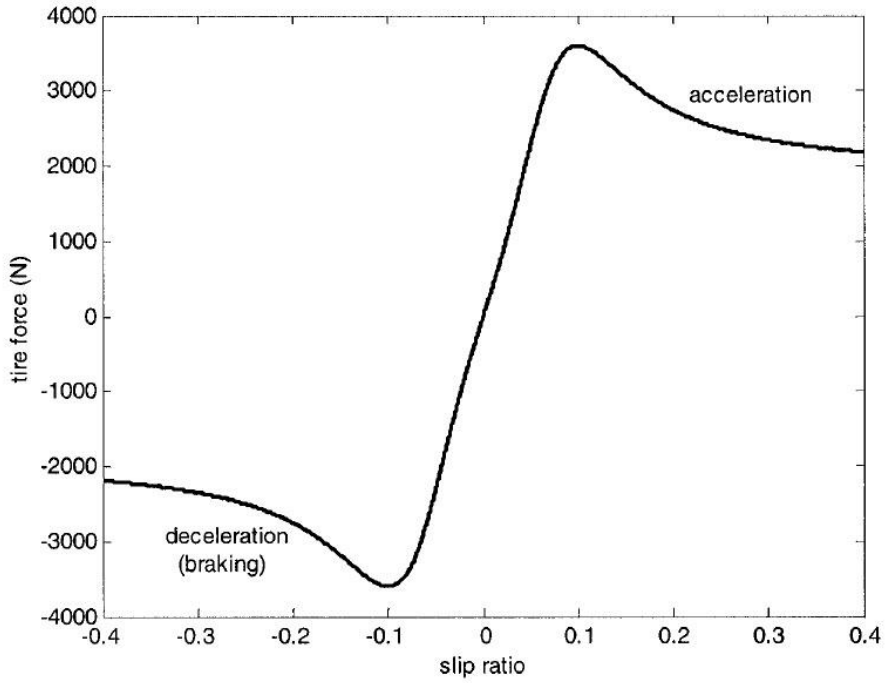

Figure 2.6 Longitudinal Tire Force as a Function of Slip Ratio

A Simulink tire block simulates a tire as a rigid-wheel, flexible-body combination in contact with the road, including only longitudinal motion. Figure 2.7 shows the dynamics and motion of a tire model used in the Simulink library, which is for a driving wheel. Figure 2.8 shows different situation when the wheel is a following wheel.

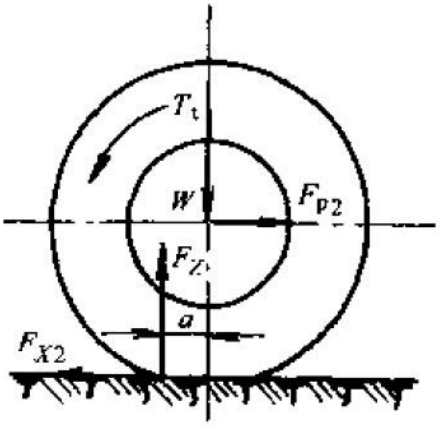

Figure 2.7 Tire Dynamics and Motion on Driving Wheel

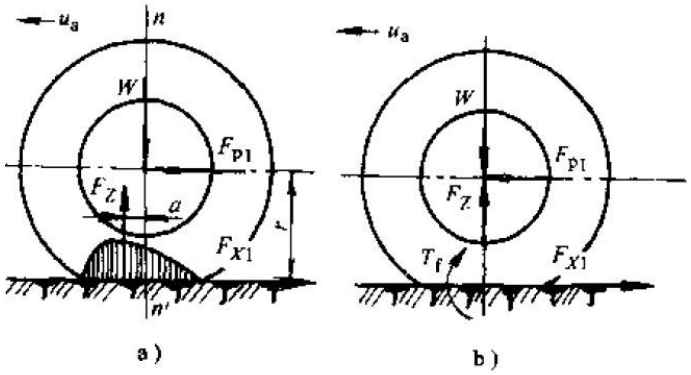

Figure 2.8 Tire Dynamics and Motion on a Following Wheel

When wheels are rolling forward, the half on the moving direction side of the tire gets pressed more than the other half, causing more deformation on that side [11]. Therefore the applying point of the force F_Z, sum of the forces from the ground, gets deviated from the central line n-n' by a distance of α. This effect forms a torque called rolling resistance torque,

$$T_f = F_Z \cdot \alpha \tag{2.15}$$

Applying force analysis to the wheel in Figure 2.8, the sum of the driving torque generated by F_{pl} must be equal to the sum of the resistant torque,

$$F_{pl}r = T_f \tag{2.16}$$

then from (2.15)

$$F_{pl} = \frac{T_f}{r} = F_Z \frac{\alpha}{r} \tag{2.17}$$

where F_Z is the vertical load, α is the deviation of F_Z from the central line of the wheel and r is the effective wheel radius. Let $f = \frac{\alpha}{r}$, therefore $f = \frac{F_{pl}}{F_Z}$ which is also called rolling resistance coefficient.

Figure 2.7 shows the forces analysis of a driving wheel. F_{X2} is the reaction of the force generated by driving torque T_t. F_Z is the same force mentioned earlier in Equation 2.17 and α is the deviation distance due to tire deformation, therefore a torque T_f is generated. Assume that the wheel inertia is I_w, we have the wheel model for the driving wheel as follows,

$$F_{X2}r_{eff} = T_t - T_f - I_w \frac{d\omega_w}{dt} \tag{2.18}$$

For the non-driving wheel,

$$I_w \frac{d\omega_w}{dt} = -F_{X1}r_{eff} - T_f \tag{2.19}$$

Equations 2.13, 2.14, 2.18 and 2.19 mathematically describe the dynamic and motion of vehicle tires used in the simulation [19].

The effective tire radius r_{eff} is calculated from the static tire radius r_{stat} and the actual wheel radius without load r_w and can be represented as

$$r_{eff} = \frac{sin\left[cos^{-1}\left(\frac{r_{stat}}{r_w}\right)\right]}{cos^{-1}\left(\frac{r_{stat}}{r_w}\right)} \cdot r_w \tag{2.20}$$

Now the following relationship is shown as $r_{stat} < r_{eff} < r_w$. The total longitudinal force is given by

$$F_x = F_{X1} + F_{X2} \tag{2.21}$$

2.4. Model verification

Close the velocity loop of the dynamic model, and then set a step input as reference. The configuration is as Figure 2.9.

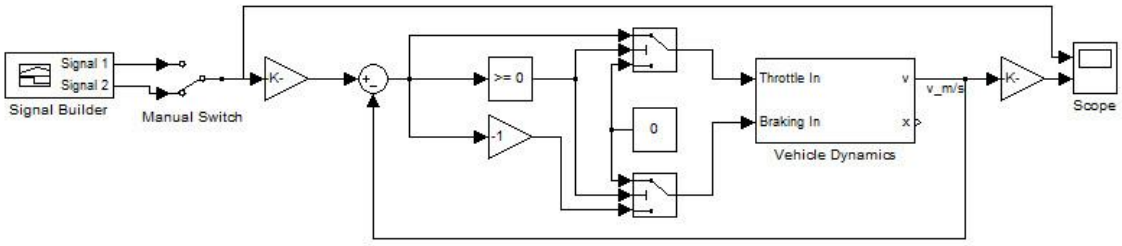

Figure 2.9 Close Loop of a Longitudinal Model

The dynamic shows step response as follows:

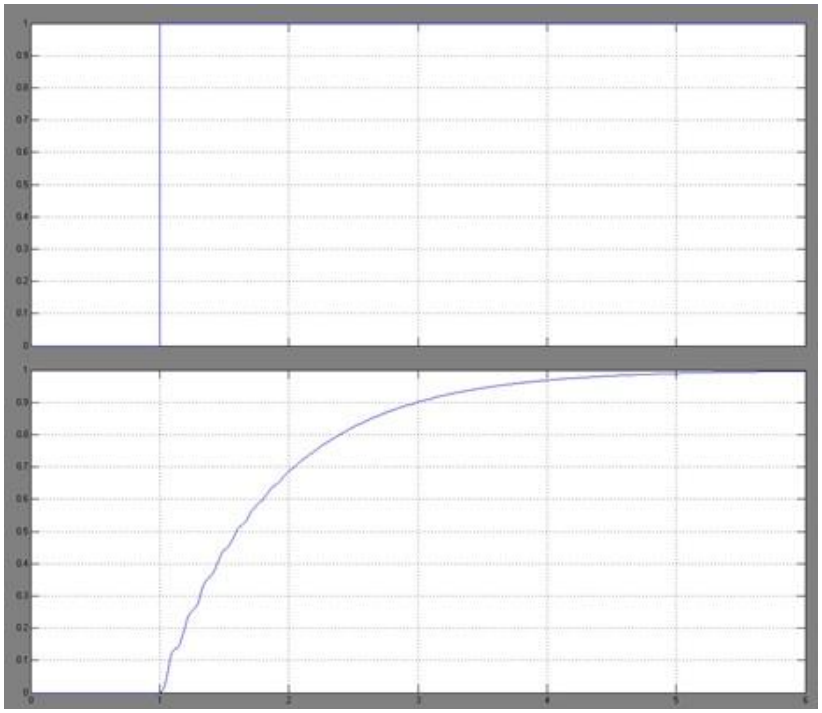

Figure 2.10 Step Response of the Close Loop Model

The response to a simple speed reference:

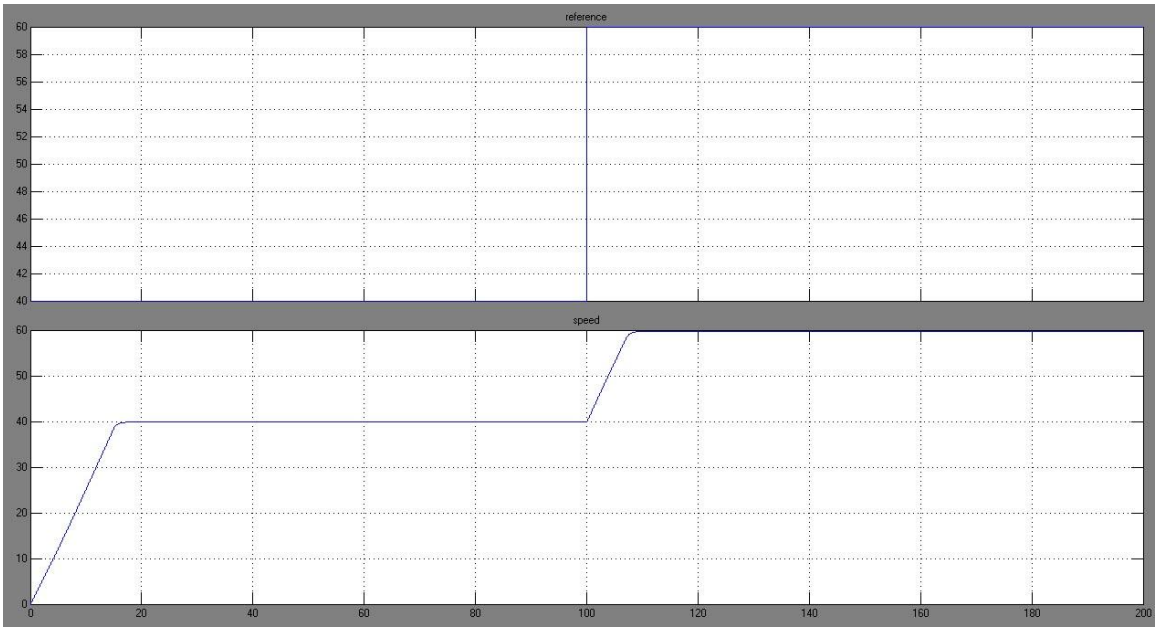

Figure 2.11 Speed Response to a Simple Speed Reference

According to the speed reference above, longitudinal and vertical tire forces have been shown in Figure 2.12:

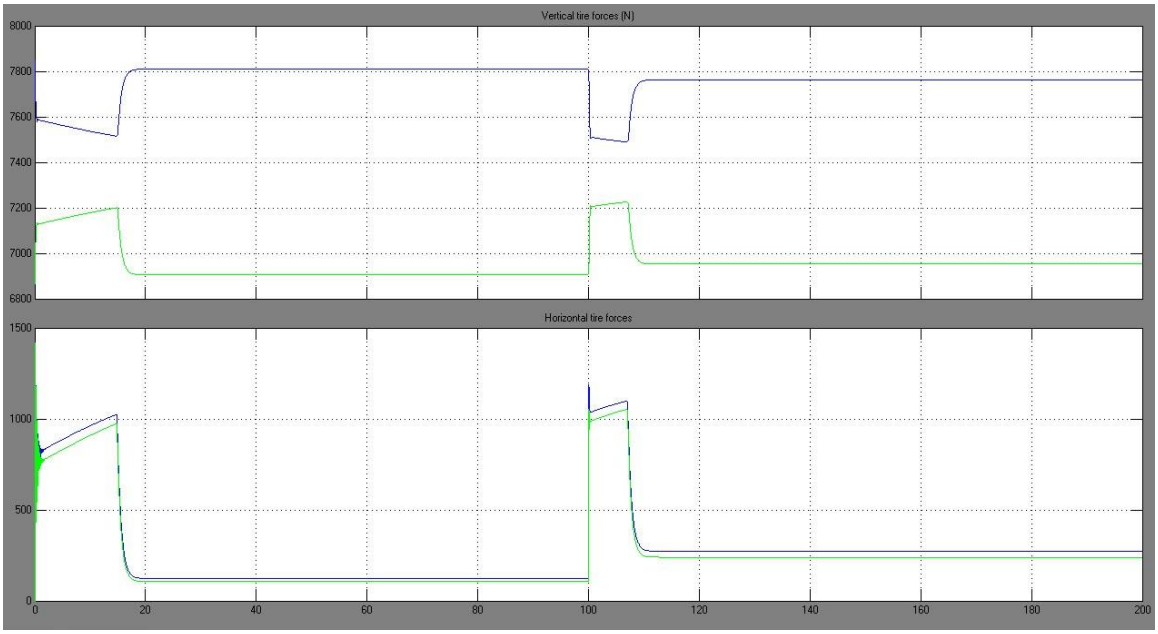

Figure 2.12 Vertical Tire Force and Horizontal Tire Force Responses

In Figure 2.12, blue lines show the forces of front wheels and green lines show the forces of rear wheels. In the upper picture, blue line shows the vertical force on the front wheel, and green line shows the vertical force on the rear wheel. In the lower picture, blue line and green line show the horizontal tire forces on the front and rear wheels respectively.

2.5. Summary

This chapter elaborates the details of a longitudinal vehicle dynamic model. Vehicle dynamics and drivetrain dynamics are described respectively. The vehicle dynamic equations depend on the longitudinal tire forces, aerodynamic drag forces, rolling resistance force and gravitational force. The longitudinal drivetrain dynamics consist of the internal combustion engine, the torque converter, the transmission and the tire dynamics.

3. ACC CONTROLLER DESIGN

3.1. Introduction

ACC (Adaptive Cruise Control) system is an extension of the standard cruise control system that takes control of the vehicle speed and tries to maintain a pre-set velocity by the driver. For ACC operation, radars or other type of detection sensors such as a lidar are used to accomplish the function that consistently measures the distance to a preceding in-lane vehicle. The sensor is integrated into the subject vehicle, shown in Figure 3.1. The ACC controller processes the kinematic information of the preceding in-lane vehicle to autonomously control the brake and throttle system to regulate the vehicle speed.

When no preceding in-lane vehicle is detected or is sufficiently apart from the subject vehicle, the ACC controller works the same way as a conventional cruise controller does. Once a preceding vehicle is detected, the ACC controller determines whether or not the subject vehicle can continue running safely at the current driver selected set-speed. If a potential hazardous condition is assessed, such as when the preceding vehicle is moving at a slower speed, or the distance between the subject vehicle and the preceding vehicle is getting too close, the ACC controller will switch from speed control mode to headway control mode. During headway control mode operation, in order to maintain a desired headway for the subject vehicle, both throttle and brake are used.

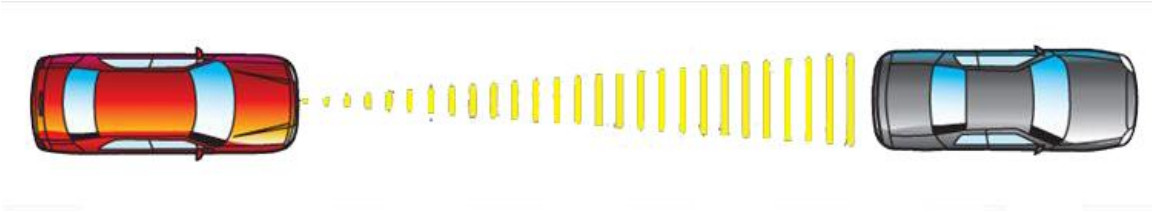

Figure 3.1 ACC System in Action

An important function of an ACC controller is to maintain a desired headway distance between the subject vehicle and preceding in-lane vehicle to reduce potential hazardous events from taking place. An ACC system also provides better driving experience and comfort by allowing the system to take control of the vehicle, which is an extension of the conventional cruise control system. Different from Automated Highway System, the ACC system is an autonomous system that doesn't depend on either wireless vehicle-to-vehicle communication or communication between vehicle and infrastructure.

Besides the two operational modes, the ACC controller would also have to decide the condition of when and where to switch between the two modes. Thus, a transitional switching logic that decides which ACC control mode should be activated has to be designed, according to different traffic situations.

This chapter will focus on the design of transitional switching logic; the next chapter will focus on the string stability analysis of ACC controlled vehicles while operating in a platoon traffic scenario.

3.2. Problem Description

Figure 3.2 shows the basic concepts based on which the ACC controller design would be mathematically modeled. Two consecutive vehicles in a generic platoon traffic situation are illustrated in the figure.

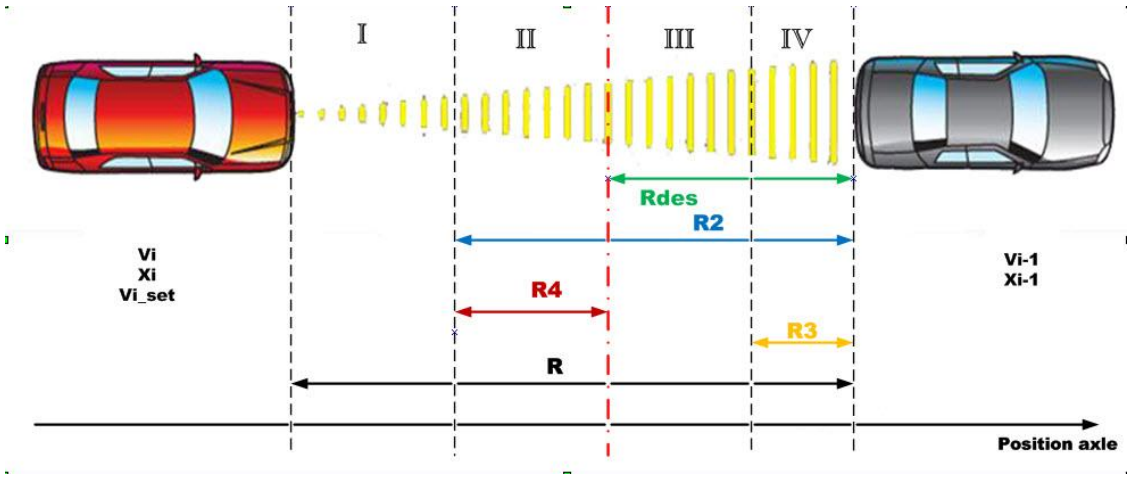

Figure 3.2 Variables Definitions for Design of an ACC Controller

v_{i-1}: Velocity of the preceding vehicle.

x_{i-1}: Relative position (based on a 1-D coordinate) of the preceding vehicle.

v_i: Velocity of following vehicle (subject vehicle).

x_i: Relative position of following vehicle (subject vehicle).

v_{i_set}: Pre-set reference speed of the following vehicle by driver.

R: Actual distance between two consecutive vehicles.

R_{des}: Desired headway distance between the two vehicles.

R_2: Switching range by which ACC controller switches between the two modes.

R_3: Braking range, in which the following vehicle has to apply maximum braking to avoid potential collision.

R_4: Buffer zone before reaching the equilibrium point.

I: Speed control zone.

II: Headway control zone.

III: Moderate Braking zone.

IV: Maximum Braking zone.

The headway control problem can be described as to develop a system that maintains a desired headway distance R_{des}, between two consecutive vehicles by modulating the speed of the following vehicle, as shown in Figure 3.2.

Once the onboard sensor of the following vehicle detects the presence of a preceding vehicle and the ACC system is engaged, the ACC control strategy starts to take control of the vehicle.

When the following vehicle reaches Zone I in Figure 3.2, the system determines there is still enough distance left from the preceding vehicle, then according to the driver pre-set speed, the controller maintains the pre-set speed as a conventional cruise controller. If the pre-set speed is greater than that of the preceding vehicle, the range between the two vehicles is going to gradually shrink, that means, the following vehicle is catching up with the preceding one.

After the following vehicle reaches Zone II, the ACC controller switches from speed control mode to headway control mode. The line between Zone II and Zone III indicates the desired distance.

There are basically two different strategies to control the velocity of the following vehicle, based on different definitions of the desired headway distance R_{des}. The different definitions of R_{des} will result in totally different results. The controller regulates the speed of the following vehicle to catch up and then maintain the desired distance R_{des}, depending on the preceding vehicle kinematic information available to the following vehicle's onboard controller as provided by the detection sensors.

In a cut-in case, if the following vehicle's onboard ACC controller detects a cut-in vehicle that causes the range R is within Zone III, the ACC controller will switch to headway control instantly and reduce the following vehicle's speed, which enlarges the

range R to be equal to R_{des}. In extreme cases when the actual range R is within Zone IV, maximum braking would be applied to avoid a potential collision.

3.2.1. Constant Headway Distance Strategy

Constant headway distance strategy simply means that regardless of the velocity of the preceding vehicle or that of the following vehicle, the desired headway distance R_{des} from the subject vehicle to the preceding vehicle to be a constant. Previous work has shown that this control strategy is not suitable for autonomous control applications such as ACC because it has been proven to be unstable in vehicle string scenario [8].

3.2.2. Constant Headway Time Strategy

A constant headway time strategy refers to a headway control condition that tries to maintain a constant headway time "h". In this case, the desired headway distance R_{des} is not a constant but a linear function of either the velocity of preceding vehicle or that the following vehicle [20]. Both situations will be discussed in this thesis.

The famous "Two Second Rule" is an example of this headway strategy. It's a rule by which a driver may maintain a safe following distance at any speed. The rule states that a driver should stay at least two seconds behind any vehicle that is directly in front of the driver's vehicle. In this case, the two second is the constant headway time mentioned above.

For drivers, the "two second" headway time rule inherently includes human response time. However, with the incorporation of an onboard controller system, the response time is much shorter than that of the human's. As such, in many ACC system implementations, multiple timed-headway gap settings are offered to the driver, typically ranging from 1 second to 2.2 seconds. The driver is allowed to select the appropriate headway setting based upon personal preferences and traffic density.

3.3. Range Vs. Range-rate Chart

A Range (*R*) versus Range-rate (*dR/dt or Rdot*) chart can be used to describe the control mode switching logic problem more efficiently and effectively [21]. Relative position and relative velocity between the two consecutive vehicles can be represented in such chart. Define variables as follows,

$$R = x_{i-1} - x_i \tag{3.1}$$

$$R_{dot} = \frac{dR}{dt} = v_{i-1} - v_i \tag{3.2}$$

At the steady state equilibrium point, the range *R* would be equal to the desired headway distance R_{des} and the velocity of the following vehicle v_i would be equal to the velocity of the preceding vehicle v_{i-1}.

3.3.1. Properties of the Range Vs. Range-rate Chart

Certain properties need to be elaborated before any mathematical formulation is developed on the *R-Rdot* chart. Figure 3.3 shows a basic principle concerning the direction of trajectories as time increases.

In the upper left quadrant, because $R_{dot} < 0$, that means $v_{i-1} < v_i$ and the following vehicle is moving faster than the preceding vehicle. In this situation, the trajectories on the *R-Rdot* chart have the tendency to go downward since the value *R* tends to decrease.

In the upper right quadrant, because $R_{dot} > 0$, that means $v_{i-1} > v_i$ and the following vehicle is moving slower than the preceding vehicle. In this situation, the trajectories on the *R-Rdot* chart have the tendency to go upward since the value *R* tends to increase.

Possible equilibrium point on the *R-Rdot* chart should be on the vertical axis, where $R = R_{des}$ and $R_{dot} = 0$.

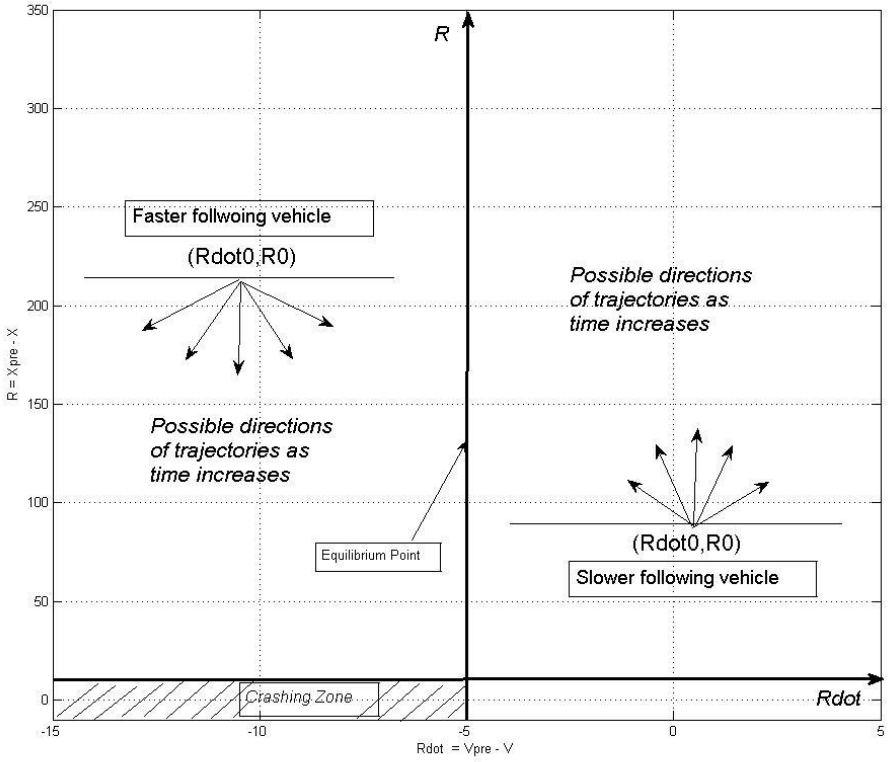

Figure 3.3 Properties of R-Rdot Chart

Another important property is shown in Figure 3.4. The chart shows two paths, path a and path b, both from an initial point (*Rdot0, R0*) to the final point (*0, Rdes*), which is the equilibrium point on the vertical axis. Intuitively, at each value of *R*, the value of *Rdot* is greater on path *b* than on path *a*, which means the velocity of the following vehicle is faster in situation of path *b* than that of path *a*. This leads to a faster elapse time on path *b* than on path *a* to travel from initial position to the end.

Quantitatively speaking, the time needed to slide from initial point to the final point would be

$$t_e = t - t_0 = \int_{R_0}^{R} \frac{dR}{R_{dot}} \tag{3.3}$$

At each value of *R*, *Rdot* on path b is greater or equal to that on path *a*, therefore the value of t_e on path *b* should be less than that on path *a*.

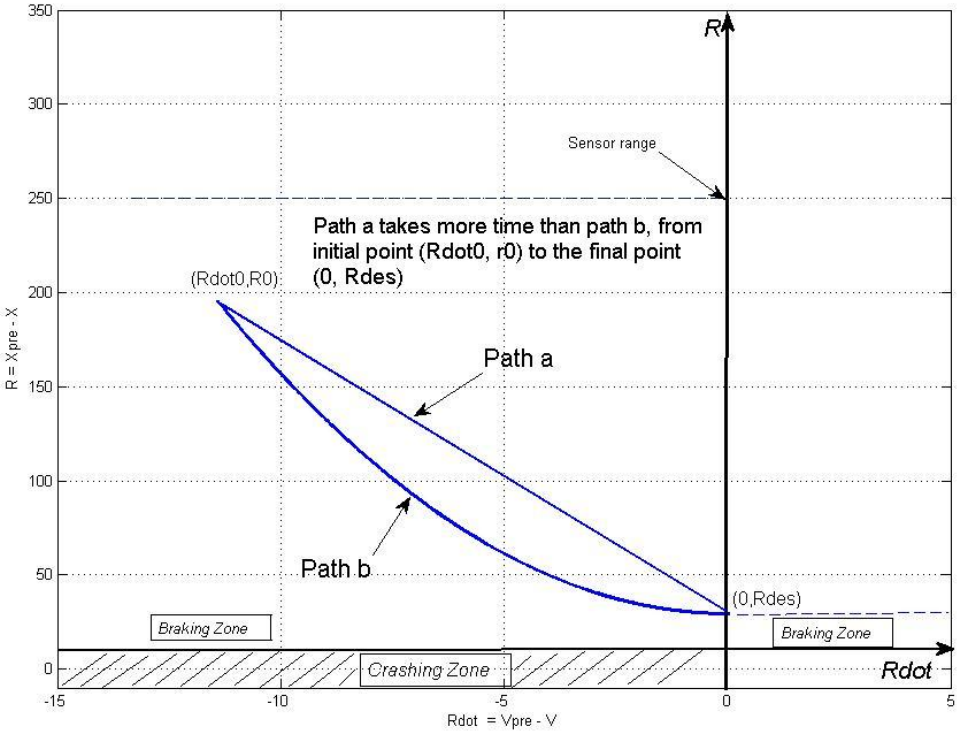

Figure 3.4 Different Paths with Different Elapsed Time

Some basic elements of the headway control problem can be easily displayed in a *R-Rdot* chart, as shown in Figure 3.5. The desired headway range and the velocity difference between consecutive vehicles can be indicated by point *(0,* R_{des} *)* located on the vertical axis, corresponding to the equilibrium position in Figure 3.2 where the actual range between the following vehicle and the preceding vehicle *R* is equal to R_{des} and the two vehicles both operate at the same speed. When the condition *Rdot* is equal to 0 *(dR/dt = 0)*, it means the range between consecutive vehicles becomes a constant.

3.3.2. A Linear Relationship between R and Rdot

The zones (Zone I, Zone II, Zone III, and Zone IV) and ACC control modes (speed control & headway control) represented in Figure 3.2 can be correspondly mapped to the R-Rdot chart of Figure 3.3. Furthermore, the boundaries of each zone indicate the switching surface that different control strategy is needed to achieve corresponding control goal. Quantitative descriptions are going to be explained in this section to gain a better understanding of the chart. A whole set of switching strategies for design of ACC controller will be represented using this chart later.

First of all, a comparison between Figure 3.2 and Figure 3.7 is necessary. Figure 3-2 shows the image of *R-Rdot* linear relationship in an intuitive way whereas Figure 3.7 shows the relationship in an *R-Rdot* chart. Since the distance R4 in Figure 3.6 serves as a buffer before the equilibrium position, then Zone II is called the buffer zone. By definition, $R = R5 + R4 + R_{des}$. While operating in Zone I (R5), the following vehicle keeps running at the pre-set speed v_{set}. Once the following vehicle proceeds into Zone II, control strategy switches from speed control mode to headway control mode and continues to approach the equilibrium point R_{des}.

The above situation can be represented by one of the three trajectories in Figure 3.7. Take trajectory 1 for example. The initial position in the space is located on the "Initial Position Line" shown in the chart. Then as the following vehicle keeps approaching the preceding vehicle at the driver's pre-set speed over R5, the state position goes downward vertically along the trajectory in the chart, until it reaches the switching surface. After passing the switching surface, the following vehicle switches from speed control mode to headway control mode. Trajectory 2 and trajectory 3 are both similar processes with different initial position and different values of R5 and R4.

Since only two vehicles are considered in this case, we can redefine $v = v_i$ and $v_p = v_{i-1}$.

Assume

$$R4 = c \cdot (v_p - v) = c \cdot R_{dot} \tag{3.4}$$

where c is a constant. Then rewrite Equation 3.4 as:

$$c = \frac{R4}{R_{dot}} = tan\,\theta < 0 \tag{3.5}$$

where $\tan\theta$ is the slope of the switch surface.

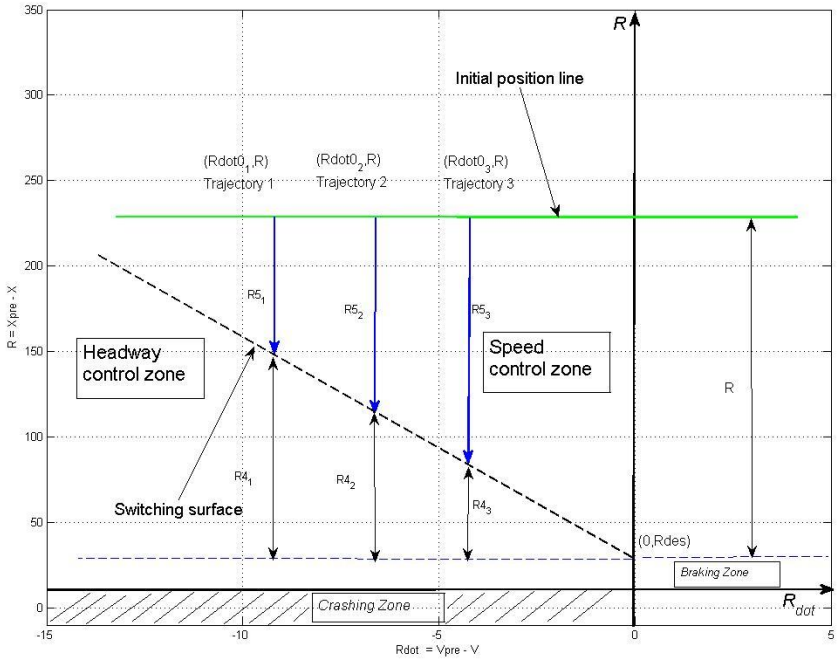

Figure 3.5 Comparison of Linear Relationship between R and Rdot

Trajectories based on linear relationship between R and Rdot have been studied as a prototype headway control system [22]. After passing through Zone I, which is segment AB in Figure 3.6, the state (*Rdot*, *R*) in the space moves along a trajectory with linear relationship between *R* and *Rdot*, which is segment BC in this case, then finally tries to reach the equilibrium point of C*(0, R_{des}).*

The equation of the trajectory BC is as follows:

$$R = -c \cdot R_{dot} + R_{des} \tag{3.6}$$

where -c is the slope of the segment BC in Figure 3.6. Obviously c should be greater than 0 here, and is different from Equation 3.5 because of the additional minus sign in Equation 3.6.

Rewriting Equation 3.6 as a general first order differential equation with the initial condition $R = R_0$, we have the following equation:

$$R = c\frac{dR}{dt} + R_{des} \tag{3.7}$$

Solving Equation 3.7 with the initial condition, one obtains

$$R = R_0 \cdot e^{-t/c} + R_{des}\left(1 - e^{-t/c}\right) \tag{3.8}$$

where c is like a time constant that decides how fast the system would approach the equilibrium point. However from the solution, it is clear that no matter how long it takes, the system would only approach the final position but would never reach it because of the exponential term in Equation 3.8. However, from a practical consideration, at $t = 5c$ time, the system will get close enough to the equilibrium point, with over 99% of the whole length of segment BC.

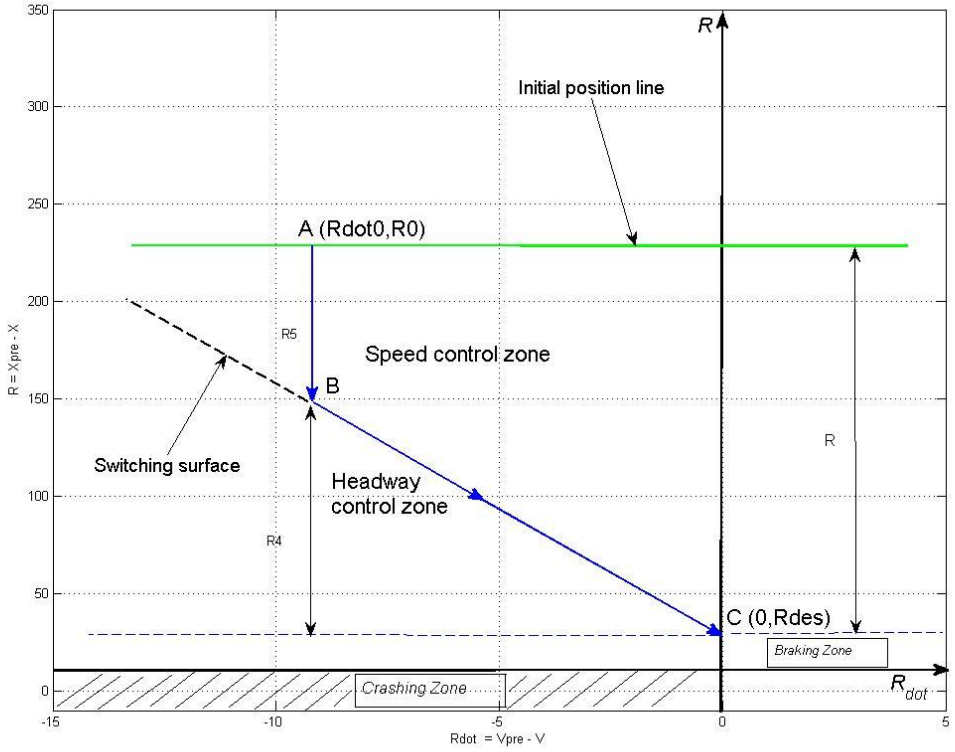

Figure 3.6 Linear Trajectory in R-Rdot Chart

3.3.3. Constant Decelerations of The Following Vehicle

This approach is to modulate the acceleration/deceleration of the following vehicle to be a constant while the following vehicle is approaching the preceding vehicle. Assume the preceding vehicle runs at a constant speed during this process. Let us define the following notations:

R_{dot0}: Initial value of R_{dot}, which is the velocity difference of the two vehicles.

R_0: Initial value of *R*, which is the headway distance between the two vehicles.

v: Velocity of the following vehicle, with initial value v_0.

v_p: Velocity of the preceding vehicle, with initial value v_{p0}.

D: Deceleration level of the following vehicle. *(D>0)*

t_e: Elapsed time during the deceleration process.

From the definitions and assumptions above,

$$v = v_0 - D \cdot t_e \tag{3.9}$$

$$v_p = v_{p0} \tag{3.10}$$

From equations 3.1, 3.2, 3.9 and 3.10,

$$R_{dot} = R_{dot0} + D \cdot t_e \tag{3.11}$$

where R_{dot0} is the initial value of R_{dot} on the trajectory.

From Equation 3.11

$$t_e = \frac{R_{dot} - R_{dot0}}{D} \tag{3.12}$$

which is the estimated amount of time needed for the following vehicle to reach the equilibrium point. In the *R-Rdot* chart, it also represents the time needed for the states to move from the initial point to the end of the trajectory, where $R = R_{des}$ and $R_{dot} = 0$. Therefore, if let $R_{dot} = 0$ in Equation 3.12,

$$t_e = \frac{-R_{dot0}}{D} \tag{3.13}$$

Equation 3.13 shows the time elapsed (for *Rdot<0*) in reaching the vertical axis, i.e., *Rdot=0*.

Rewriting Equation 3.11 as,

$$\begin{aligned} & R_{dot} = R_{dot0} + D \cdot t_e \\ \Leftrightarrow & \frac{dR}{dt} = R_{dot0} + D \cdot t_e \\ \Leftrightarrow & dR = R_{dot0} dt + D \cdot t dt \end{aligned} \tag{3.14}$$

then integrating the two sides of Equation 3.14 with respect to time,

$$\int_{R_0}^{R} dR = \int_{0}^{t_e} R_{dot0} dt + \int_{0}^{t_e} D \cdot t dt$$

$$R - R_0 = R_{dot0} \cdot t_e + D \cdot \frac{1}{2} t_e^2 \tag{3.15}$$

Substituting t_e in Equation 3.15 with Equation 3.12 and rearranging the two sides, we obtain

$$R - \frac{R_{dot}^2}{2D} = R_0 - \frac{R_{dot0}^2}{2D} \tag{3.16}$$

When the following vehicle reaches equilibrium point, $R_{dot} = 0$, R is expected to be R_{des}, which means Equation 3.16 should be equal to R_{des},

$$R - \frac{R_{dot}^2}{2D} = R_{des}$$

$$R = \frac{R_{dot}^2}{2D} + R_{des} \tag{3.17}$$

Therefore a relationship between *R* and *Rdot* has been derived and shown in Figure 3.7. Depending on how large the value of deceleration would be, the elapsed time of the deceleration process can be calculated by Equation 3.13. When a larger deceleration level is selected, the trajectory of the deceleration process is shifting toward the more negative side of *Rdot*, which is shown in Figure 3.8.

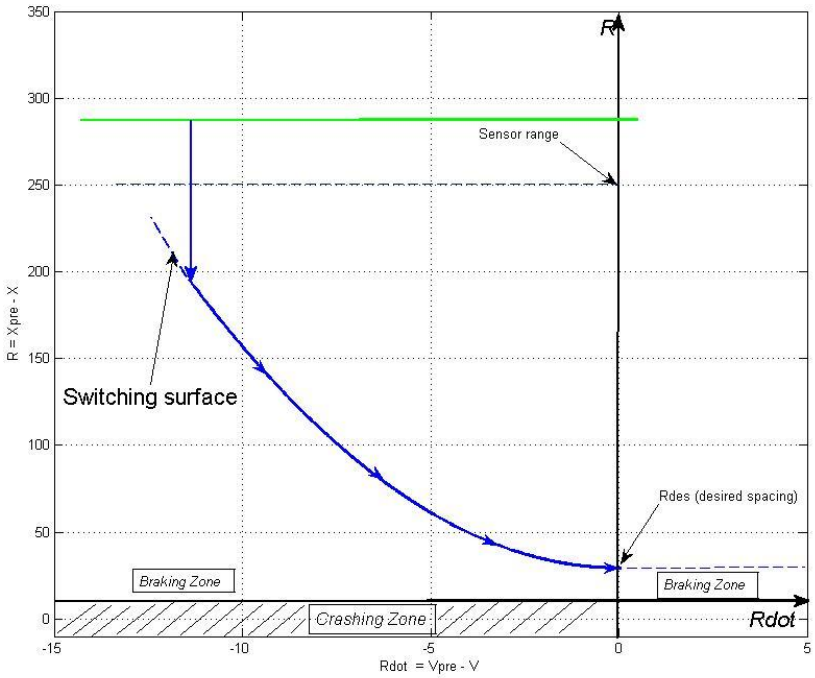

Figure 3.7 Trajectory of Constant Deceleration Strategy

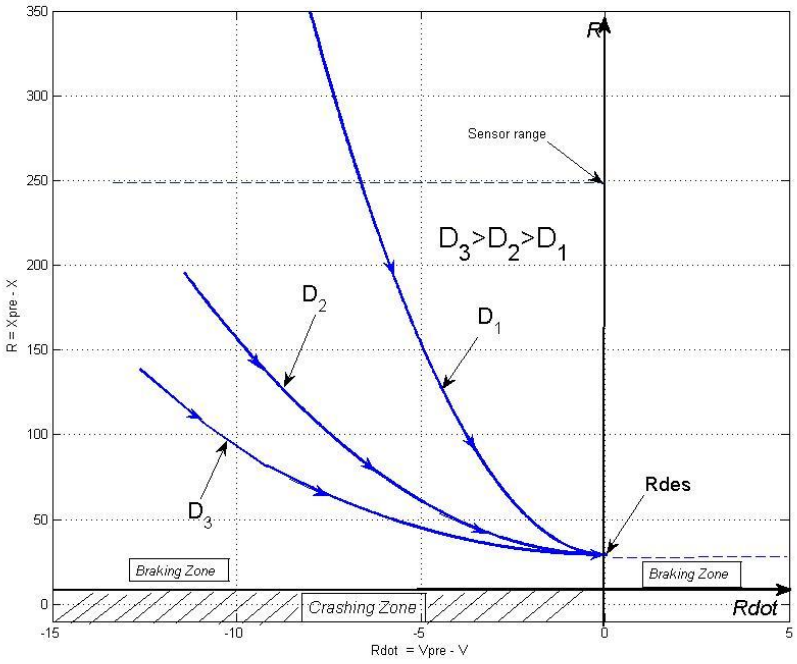

Figure 3.8 Trajectories with Different Deceleration Level

3.4. Design of A Headway Control Strategy

Assumptions had been made that a reliable conventional cruise control system had already been available to represent the speed control mode and the simulation has been conducted in a situation in which the preceding vehicle is moving at a constant speed for most of the time. A desirable comparison can only be made when the desired headway distance, i.e., R_{des} is fixed in the *R-Rdot* chart.

With reference to Figure 3.9 below, the design process proposed in this thesis consists of the following steps:

- Define the desired headway distance for a selected velocity and headway time. For example, define $R_{des} = h \cdot v_p$, where h is called headway time with second as its unit and v_p is the velocity of the preceding vehicle. Usually R_{des} is a function of either the velocity of the preceding vehicle or

that of the following vehicle. (A comparison will be presented in the next section.) In this example, h is set to be 1.5sec, v_p is set to be the velocity of a lead vehicle which follows a constant speed profile, starting roughly at *17.88 m/s, i.e., 45 MPH*.

- Choose the deceleration to be used. Assumption has been made that the maximum deceleration which human drivers feel comfortable with is $0.3g$, in the simulation used by this thesis, the maximum comfortable deceleration is set to be $D1 = 0.2g$, where $g = 9.8\, m/s^2$. The design constant deceleration was selected to be $0.1g$.
- Construct a switching zone. After step 2, a constant deceleration parabola can be drawn on the *R-Rdot* chart. Above the parabola, a switching zone has to be constructed within which the following vehicle performs switching from speed control to headway control. The parabola in step 2 can serve as the lower limit of the switching zone. The upper limit of the switching zone could be designed to be a straight trajectory, which indicates a linear relationship of *R* and *Rdot*, as explained in Section 3.3.2, or could be another parabola trajectory, which indicates an approach by the following vehicle with constant deceleration $D2$.
- If the design doesn't involve use of brake in the approaching process, coasting deceleration *0.02g* (calculated from the simulation model) could be used to be the upper limit of the switching zone, which will result a costing down of the following vehicle's speed during the approaching process.
- Design a Dead Zone around the equilibrium point so that the trajectory won't jitter due to strict boundaries of different zones on the *R-Rdot* chart. This step will be elaborated later in this section.

The proposed control system is implemented using the vehicle model discussed in Chapter 2 in the Matlab/Simulink environment. Extensive simulations were performed and the simulation results are shown in Figure 3.9 and Figure 3.10. The initial velocities

for the preceding vehicle and the following vehicle are both 0 and the initial range between the two vehicles is set to be 300 meters. The speed profile that the leading vehicle uses as reference input is a step input with magnitude of 45 MPH, and the driver pre-set speed for the following vehicle is 70 MPH. It was assumed that ACC is activated on the following vehicle.

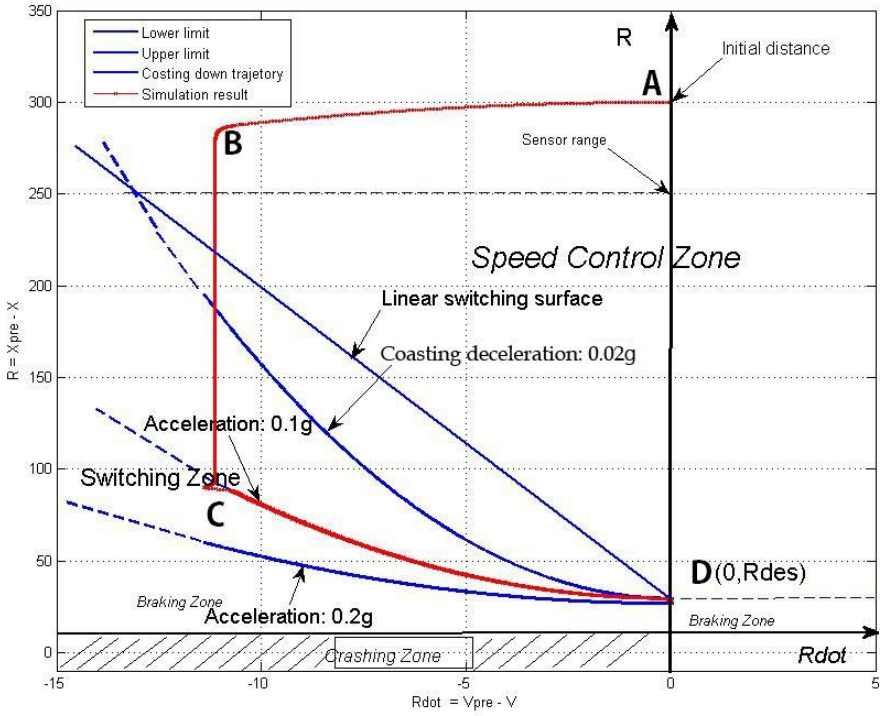

Figure 3.9 Example of an Adaptive Cruise Control Strategy Design

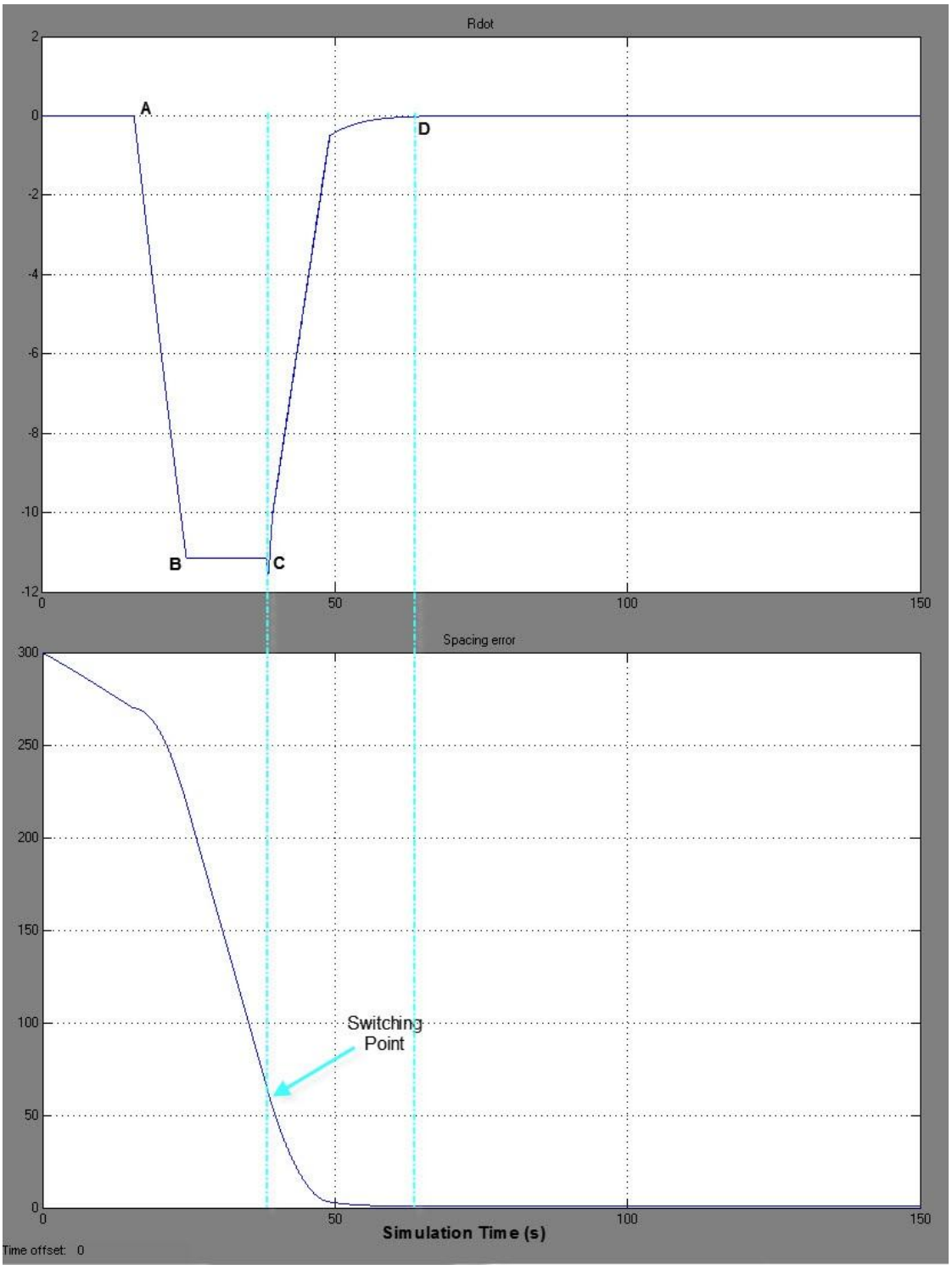

Figure 3.10 Rdot and Spacing Error during the Simulation

From Figure 3.9, it's clear that the range in between is getting shorter as time epalses. Then after a while, when the trajectory on *R-Rdot* chart crosses the switching line and gets into the switching zone, the ACC controller immediately switches from speed control mode to headway control mode and starts to decelerate with a constant deceleration of 0.1g, as designed in the example. In Figure 3.10, it shows the spacing error between the actual spacing and the desired spacing becomes smaller and smaller as time elapses and goes to zero eventually. Point A, B, C and D shown in Figure 3.10 are corresponding to points with the same name in Figure 3.9.

Another simulation case has been designed so that the preceding vehicle conducts a sudden braking during headway control mode of the following vehicle, as shown in Figure 3.11 and Figure 3.12, where y axis shows velocity input and x axis shows simulation time in seconds.

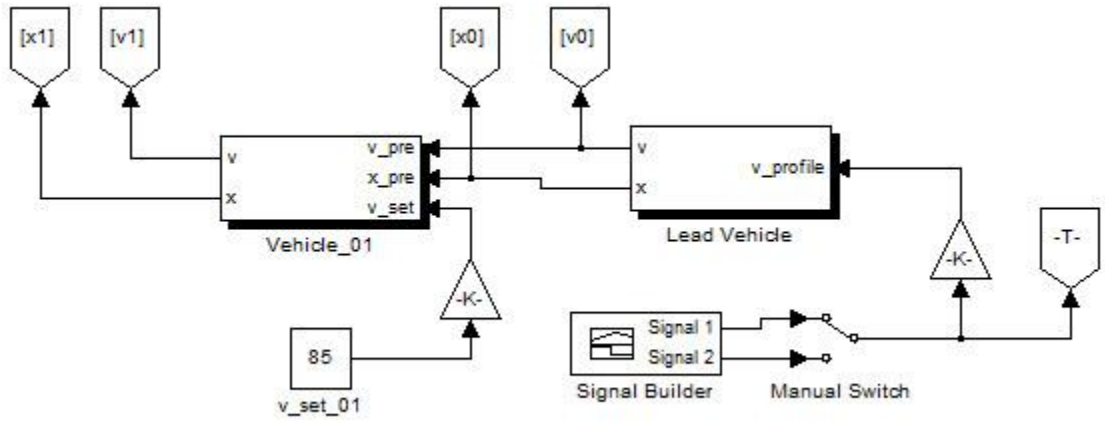

Figure 3.11 Car Following Model

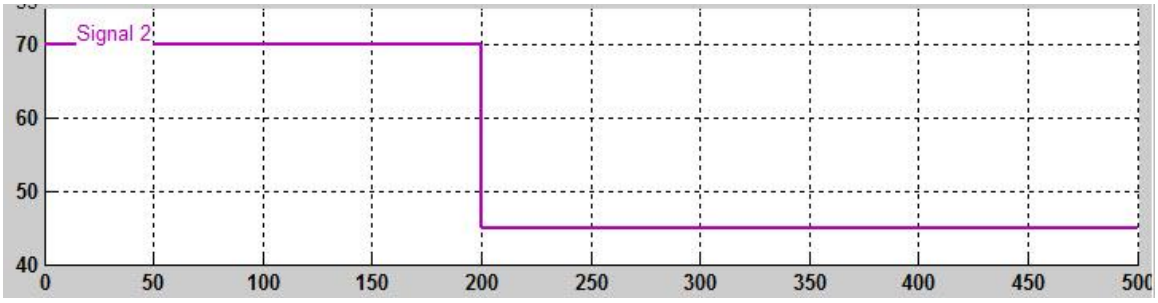

Figure 3.12 Reference Input for Sudden Braking Simulation (velocity vs. time in seconds)

The trajectory on *R-Rdot* chart is shown as Figure 3.13. It's clear that before the preceding vehicle makes the sudden braking, the trajectory of (*Rdot, R*) looks just like what has been shown before, and the equilibrium point has already been reached. Then the preceding vehicle makes a sudden brake, which slows its speed from 70 MPH to 45 MPH. Meanwhile the following vehicle's pre-set speed is set to be 85 MPH. This slowing event pushes the following vehicle into the braking zone, where the following vehicle achieves maximum braking (0.2g) authority. Eventually, the trajectory transitions back to the switching zone and slows down at a constant deceleration.

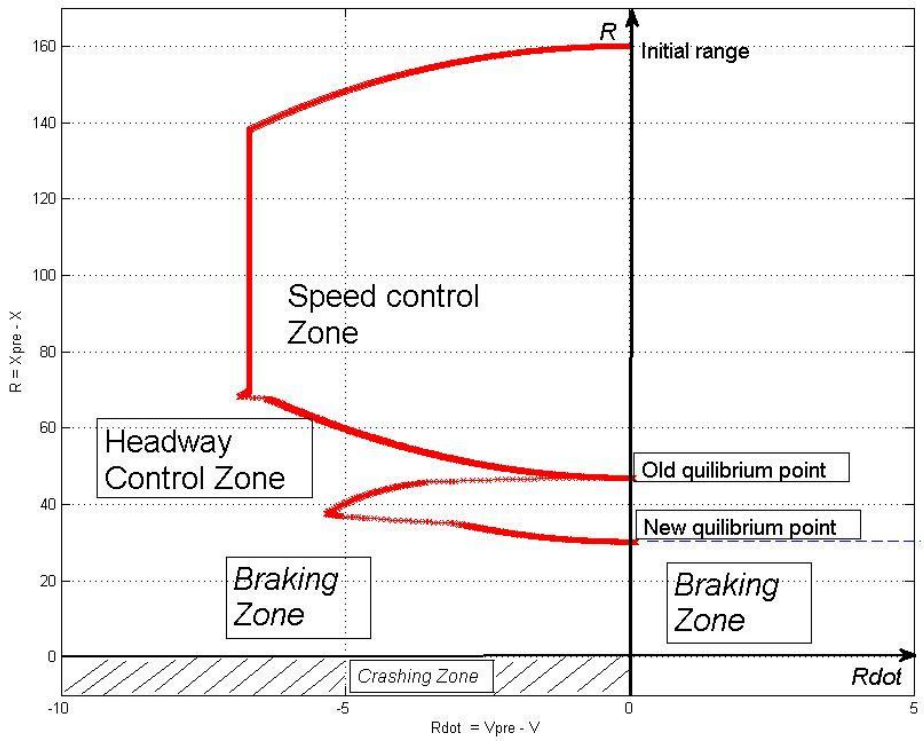

Figure 3.13 Trajectory with Sudden Braking of the Preceding Vehicle

In step 5 of the design procedures for the proposed ACC controller, a dead zone should be designed around the equilibrium point $(0, R_{des})$ on the *R-Rdot* chart. The reason for design a dead zone is because if a strict boundary is defined on the *R-Rdot* chart between two separate zones with two control strategies leading to conflicting control goals, the trajectory would be pushed back and forth within a small range on the boundary. Although from a large scale, the jittering phenomenon is hardly noticeable, it'll still become an unstable issue for the whole system when the string of ACC controlled vehicles gets longer.

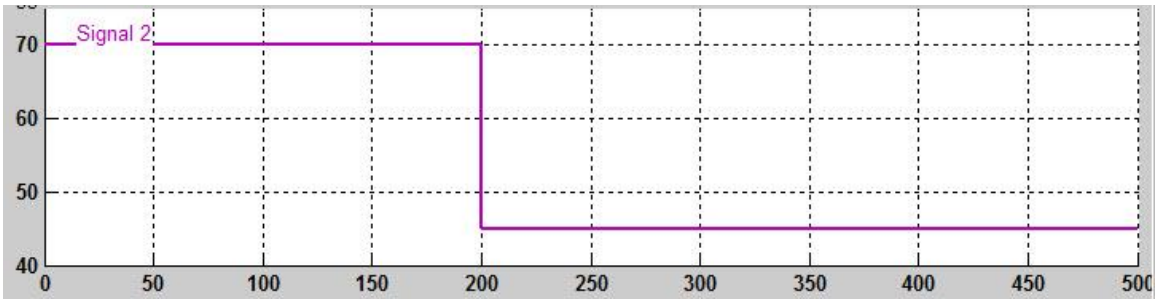

Figure 3.14 Reference for Jittering Phenomenon Example

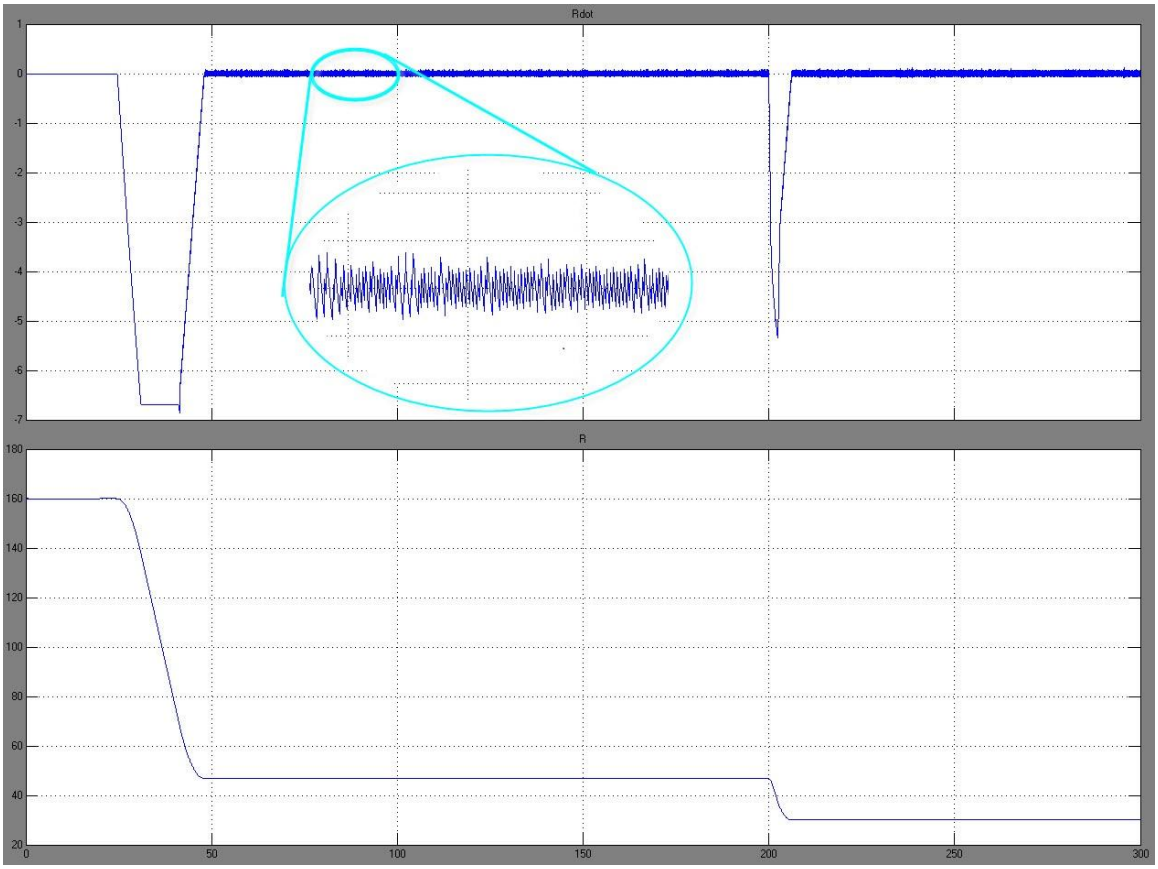

Figure 3.15 Jittering Phenomenon around the Equilibrium Point

Take the simulation above for example, whose reference input is shown in Figure 3.14. Once the trajectory hits the vertical axis, on the left side of the vertical axis, it's the headway control strategy that is in charge of the vehicle, which will push the trajectory to

the vertical axis as close as possible; however since a PD controller is used to mitigate the spacing error between the actual range of consecutive vehicles and the desired headway distance, an overshoot is always possible. Due to the overshoot of the trajectory, it could sometimes go across the vertical axis and get into the right side, within which the speed control strategy will take charge. The speed control strategy forces the vehicle speed to match the driver's pre-set speed, which is greater than the speed of the preceding vehicle because the trajectory initially comes from the left side where $R_{dot} < 0, \text{i.e.}\, v > v_p$. Therefore, the trajectory has to be pushed back to the left side of the vertical axis. After that it will repeat the process described above another round and continue within a relatively small range. It's very clear when a close-up view is taken at the *Rdot* value as time passes, separately, which is shown in Figure 3.15.

To mitigate the jittering phenomenon, a dead zone is designed around the equilibrium point, as shown in Figure 3.16. The upper limit of the dead zone is set to be $1.1\mathrm{R_{des}}$, the lower limit $0.9\mathrm{R_{des}}$ and the width 0.5 m/s for this simulation.

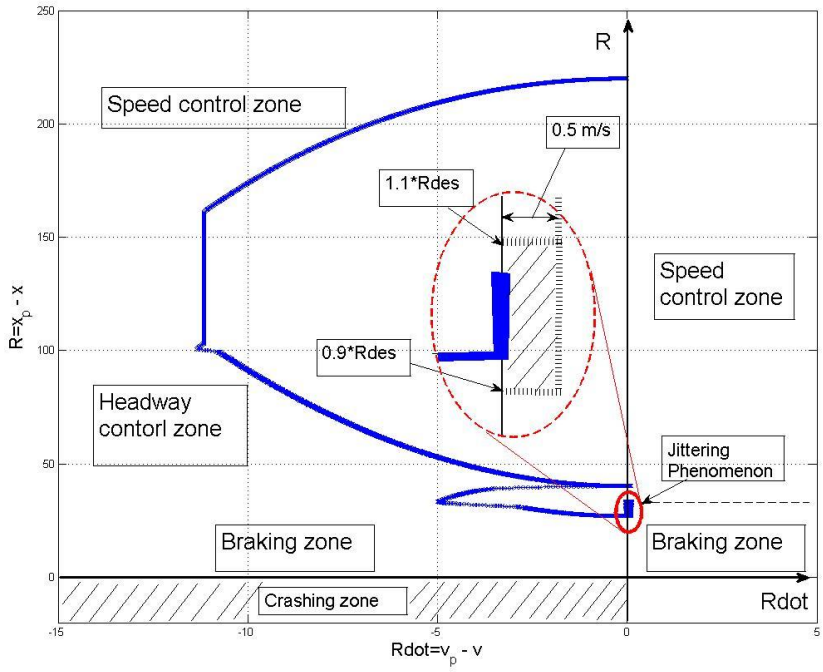

Figure 3.16 Dead Zone Design for Mitigation of Jittering Phenomenon

Within this dead zone headway control strategy applies, and speed control strategy takes over beyond it. As a result of this modification, the result became quite satisfactory, which is shown in Figure 3.17 and Figure 3.18.

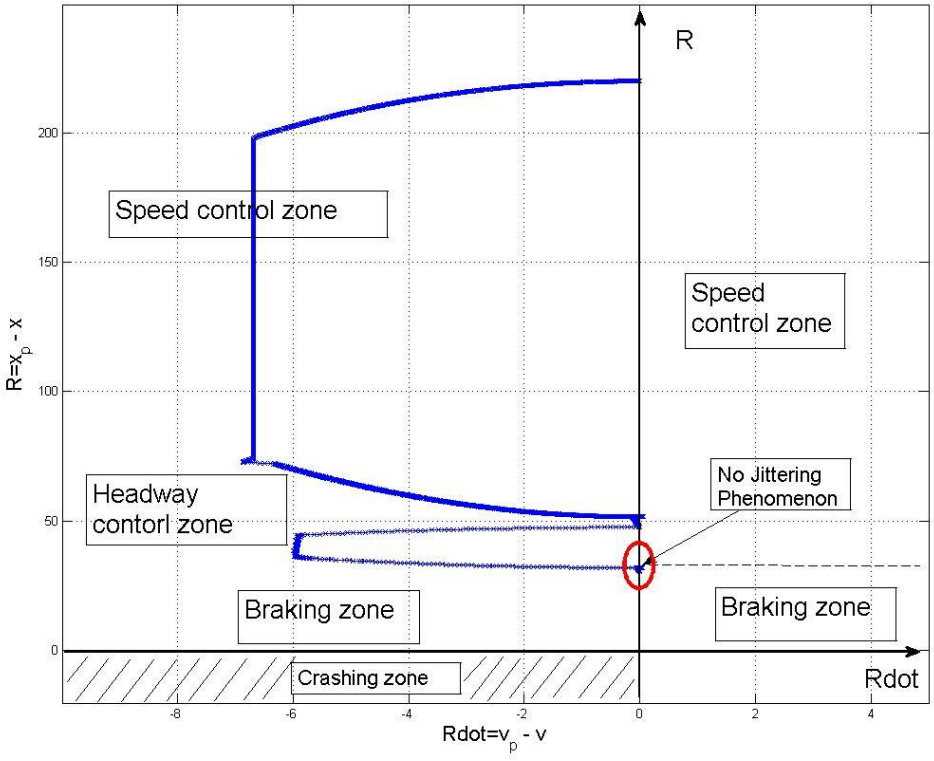

Figure 3.17 *R-Rdot* Chart Showing No Jittering Phenomenon after Design of Dead Zone

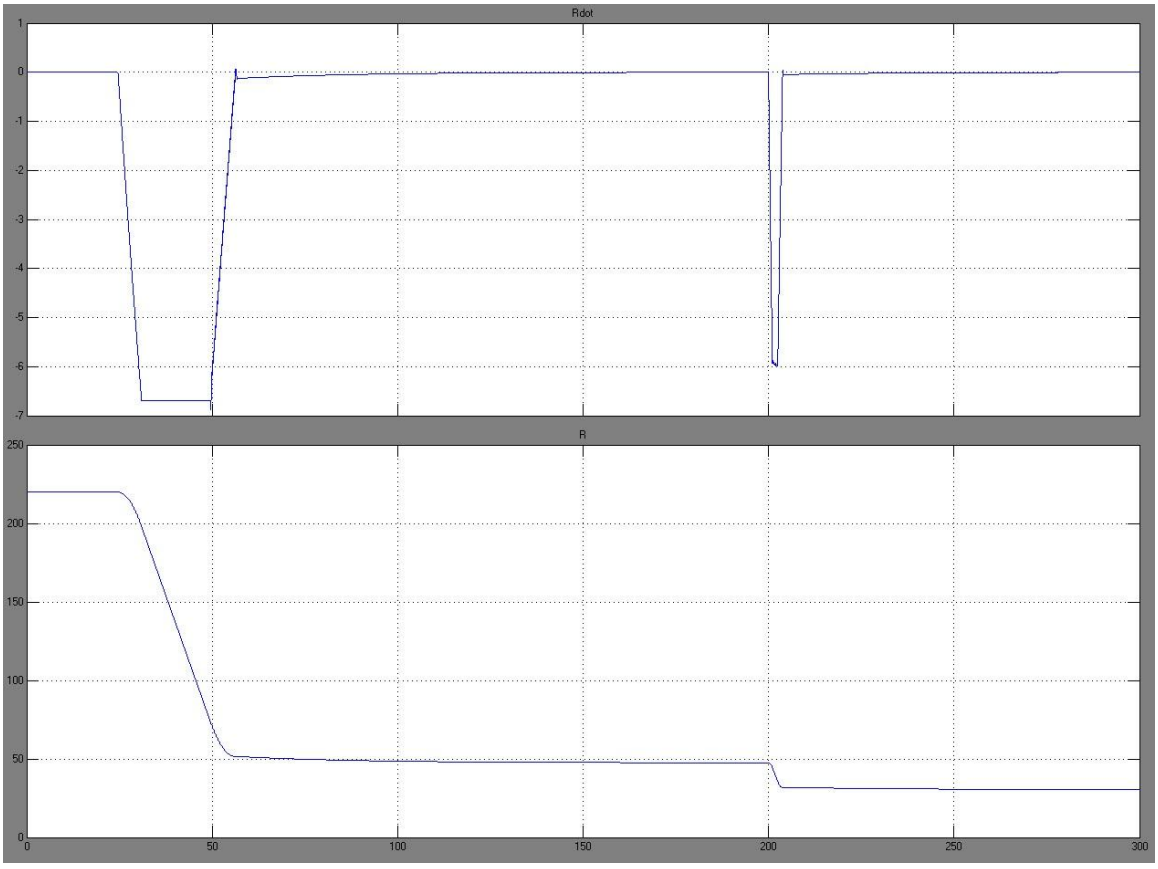

Figure 3.18 Values of R Shows Mitigated Jittering Phenomenon

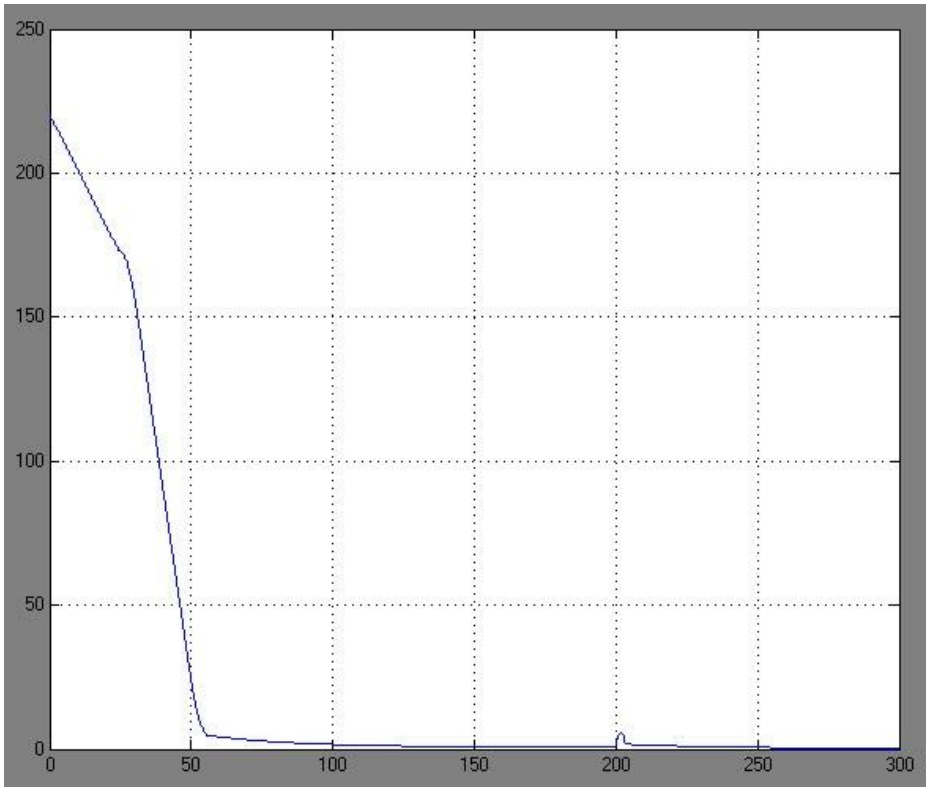

Figure 3.19 Spacing Error with Dead Zone Design

3.5. Chapter Summary

In this chapter, a systematic method has been discussed to design an ACC controller. An *R-Rdot* chart was introduced to assist the design process. Constant deceleration of the following vehicle was discussed to achieve a faster process to the equilibrium point, i.e. the desired headway distance to the preceding vehicle. Vehicle models described in the last chapter are used to implement the control strategies and the simulation results have been presented as well. A dead zone was designed to mitigate jittering phenomenon around the equilibrium point.

4. STRING STABILITY ANALYSIS

String stability issue has been addressed by other researchers after the adaptive cruise control (ACC) concept was introduced [3]. The main problem is when many ACC equipped vehicles form a vehicle platoon end to end, how the control algorithm is designed to ensure that the spacing error, which is the deviation of the actual range from the desired headway distance, would not amplify as the number of following vehicles increases downstream along the platoon.

Different spacing policies have been briefly discussed in Section 3.2, including constant spacing policy and constant headway time policy. In this chapter, these control strategies will be discussed in detail.

4.1. Introduction

Consider a platoon of vehicles equipped with ACC controller operating in headway control mode, as shown in Figure 4.1 and the notations used in the figure are stated as follows:

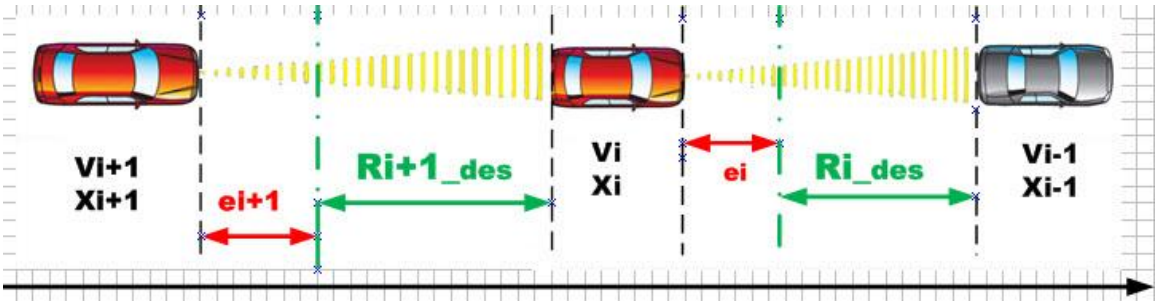

Figure 4.1 Vehicles Moving in a Platoon

v_{i-1}: Velocity of the *i-1* th vehicle.

x_{i-1}: Relative position (based on a 1-D coordinate) of the *i*-1 *th* vehicle.

v_i: Velocity of the *i*-th vehicle.

x_i: Relative position of the *i*-th vehicle.

ε_{i-1}: Spacing error of the *i*-1 th vehicle.

ε_i: Spacing error of the *i*-th vehicle.

The length of each vehicle is not going to affect the result of the analysis, thereby an assumption is made that the vehicle length is neglected in the following calculation. Relative position of each vehicle in the platoon is defined according to a common reference starting point. The mathematical definitions of these variables are given in the following sections.

4.1.1. Desired Headway Distance R_{des} Based on Preceding Vehicle Velocity

The desired spacing between consecutive vehicles is defined as a function of the velocity of the preceding vehicle:

$$R_{i\_des} = h \cdot v_{i-1} = h \cdot \dot{x}_{i-1} \tag{4.1}$$

where *h* represents the desired headway time. According to the 2 second rule, *h* should be equal to 2 seconds. However since the vehicle is controlled by ACC controller whose response time is much shorter than human driver, typically *h* could be around chosen from 1 to 2.2 second.

The spacing error of the *i*-th vehicle is defined as

$$\varepsilon_i = x_{i-1} - x_i - R_{i_{des}} \tag{4.2}$$

From Equation 4.1, Equation 4.2 can be rewritten as

$$\varepsilon_i = x_{i-1} - x_i - h \cdot \dot{x}_{i-1} \tag{4.3}$$

4.1.2. Desired Headway Distance R_{des} Based on Following Vehicle Velocity

The other way to define the desired headway distance is to set R_{i_des} as a function of the following vehicle's velocity [3, 9]:

$$R_{i\_des} = h \cdot v_i = h \cdot \dot{x}_i \tag{4.4}$$

Therefore the spacing error of the *i*-th vehicle under this definition is:

$$\varepsilon_i = x_{i-1} - x_i - h \cdot \dot{x}_i \tag{4.5}$$

In the later sections, both implementations will be discussed and a brief comparison is presented based on simulation results. String stability issues will be addressed under both definitions, respectively.

4.2. Conditions for String Stability

It is important to describe how the spacing error would propagate from vehicle to vehicle downstream along the platoon, because the spacing error of each vehicle in the platoon is expected to be non-zero during acceleration or deceleration of the preceding vehicle. Assuming that every vehicle in the platoon uses the same spacing policy, control algorithm and switching strategy, the string stability of a platoon of vehicles can be referred to as such a property that the spacing error of each vehicle is guaranteed not to be amplified as the number of vehicles in the platoon increases [9].

Mathematically, a desirable characteristic for string stability is often specified as

$$\|\varepsilon_i\|_\infty \leq \|\varepsilon_{i-1}\|_\infty \tag{4.6}$$

where ε_i is the spacing error of the *i*-th vehicle and ε_{i-1} is that of the *i*-1 th vehicle [3, 8].

Equation 4.6 implies that the least upper bound of the spacing error of the *i*-th vehicle should be less than or equal to that of the preceding one, which means the spacing error does not amply downstream along the vehicle platoon.

Previous work has shown that Equation 4.6 requires two conditions [8],

(1) $\|H(s)\|_\infty \leq 1$

(2) $h(t) > 0$

where $H(s)$ is the error transfer function in frequency domain, defined as,

$$H(s) = \frac{\varepsilon_i(s)}{\varepsilon_{i-1}(s)} \tag{4.7}$$

and $h(t)$ is the impulse response of $H(s)$.The outline of the proof of these conditions is as follows:

Proof: Let $y(t) = \varepsilon_i(t)$, $x(t) = \varepsilon_{i-1}(t)$, define $g(t)$ such that

$$y(t) = g(t) * x(t) \tag{4.8}$$

That is, $y(t)$ is equal to the convolution of $g(t)$ and $x(t)$.

Equation 4.8 can be rewritten as integration form,

$$y(t) = \int_0^t g(t-\tau)x(\tau)d\tau \tag{4.9}$$

Performing Laplace transform Equation 4.9, one obtains

$$Y(s) = G(s)X(s)$$

where $G(s) = \mathcal{L}[g(t)]$ is the transfer function of the system, and $g(t)$ is the impulse response of the system.

Define ∞-norm and 1-norm of the transfer function $G(s)$ as follows,

∞-norm: $\|G(s)\|_\infty = sup_\omega|G(j\omega)|$

1-norm: $\|g\|_1 = \int_0^\infty |g(t)|\, dt$

According to Parseval's Theorem for Fourier series, the sum (or integral) of the square of a function is equal to the sum (or integral) of the square of its transform, a.k.a. Rayleigh's energy theorem [23]. Therefore,

$$\begin{aligned} \|y(t)\|_2^2 &= \|Y(s)\|_2^2 \\ &= \frac{1}{2\pi}\int_{-\infty}^{\infty} |G(j\omega)|^2\,|X(j\omega)|^2 d\omega \\ &\le \|G(s)\|_\infty^2 \cdot \frac{1}{2\pi}\int_{-\infty}^{\infty} |X(j\omega)|^2 d\omega \\ &= \|G(s)\|_\infty^2 \cdot \|X(s)\|_2^2 \end{aligned} \tag{4.10}$$

Because $\|X(s)\|_2^2 = \|x(t)\|_2^2$ (Parseval's Theorem), Equation 4.10 can be rewritten as

$$\|y(t)\|_2^2 \le \|G(s)\|_\infty^2 \cdot \|x(t)\|_2^2 \tag{4.11}$$

Therefore,

$$\begin{aligned} \|G(s)\|_\infty^2 &\ge \frac{\|y(t)\|_2^2}{\|x(t)\|_2^2} \\ \Rightarrow \|G(s)\|_\infty &= sup_{t\in L^2} \frac{\|y(t)\|_2}{\|x(t)\|_2} \end{aligned} \tag{4.12}$$

From Equation 4.9,

$$\begin{aligned} |y(t)| &= \left|\int_{-\infty}^{\infty} g(\tau)x(t-\tau)d\tau\right| \\ &\le \int_{-\infty}^{\infty} |g(\tau)x(t-\tau)|d\tau \\ &\le \|x(t)\|_\infty \cdot \int_{-\infty}^{\infty} |g(\tau)|\,d\tau \\ &= \|g(t)\|_1 \cdot \|x(t)\|_\infty \end{aligned} \tag{4.13}$$

Since Equation 4.13 for any *t*, it's also true when $|y(t)|$ is replaced by the least upper bound of $y(t)$, that is , $\|y(t)\|_\infty$. Therefore,

$$\|y(t)\|_\infty \leq \|g(t)\|_1 \cdot \|x(t)\|_\infty \tag{4.14}$$

Equation 4.14 can be rewritten as

$$\|g(t)\|_1 = sup_{t\in L^\infty} \frac{\|y(t)\|_\infty}{\|x(t)\|_\infty} \tag{4.16}$$

String stability requires Equation 4.6. Therefore to guarantee string stability, Equation 4.16 has to be less than or equal to 1, which means

$$\|h(t)\|_1 \leq 1 \tag{4.17}$$

where $h(t)$ is the impulse response of the error transfer function $H(s)$ in Equation 4.07.

QED.

However to design a system that satisfies inequality (4.17) is not intuitive. The following lemma shows that instead of requiring condition (4.17), a system could satisfy the following two conditions to ensure string stability.

Lemma: If $h(t) > 0$, then all the input output induced norms are equal [8].
Proof: Let γ_p be the *p*-th induced norm i.e.

$$\gamma_p = sup_{t\in L^p} \frac{\|y\|_p}{\|x\|_p} \tag{4.18}$$

From linear systems theory,

$$\left|\widehat{H}(0)\right| \leq \left\|\widehat{H}(j\omega)\right\|_\infty \leq \gamma_p \leq \|h\|_1 \tag{4.19}$$

If h(t)does not change sign, then

$$\left|\widehat{H}(0)\right| = \left|\int_0^\infty h(t)dt\right| \leq \int_0^\infty |h(t)|\, dt = \int_0^\infty |h(t)|dt = \|h\|_1 \tag{4.20}$$

Therefore $\left|\widehat{H}(0)\right| = \|h\|_1$ if and only if $h(t)$ does not change sign. Hence from Equation 4.19,

$$\left\|\widehat{H}(j\omega)\right\|_\infty = \gamma_p = \|h\|_1 \tag{4.21}$$

QED.

To sum up:

Condition $\|H(s)\|_\infty \leq 1$ guarantees $\frac{\|y(t)\|_2}{\|x(t)\|_2} \leq 1$ since $\|H(s)\|_\infty = \|G(s)\|_\infty = sup_{t\in L^2} \frac{\|y(t)\|_2}{\|x(t)\|_2}$, from Equation 4.12.

Condition $h(t) > 0$ guarantees that $\|H(j\omega)\|_\infty = \|h\|_1$, implies $\|H(j\omega)\|_\infty = sup_{t\in L^\infty} \frac{\|y(t)\|_\infty}{\|x(t)\|_\infty}$, from Equation 4.16.

Therefore, if $\|H(s)\|_\infty \leq 1$ and $h(t) > 0$ are satisfied, string stability is guaranteed.

4.3. String Stability Analysis of A Vehicle Platoon

Before doing string stability analysis, the time constant of the vehicle system model in Chapter 2 has to be determined. The reason for system identification of the vehicle model is because the vehicle dynamic model described in Chapter is a highly non-linear model, and simplification has to be made before doing system stability analysis mathematically.

Usually a second order linear system can be used to represent the 1-D dynamic model of a vehicle for longitudinal control, as shown below,

$$y = \frac{1}{(\tau_1 s + 1)(\tau_2 s + 1)} u \tag{4.22}$$

Figure 4.2 shows close loop response of the vehicle model, with a step input from 0 to 1 m/s as velocity reference input.

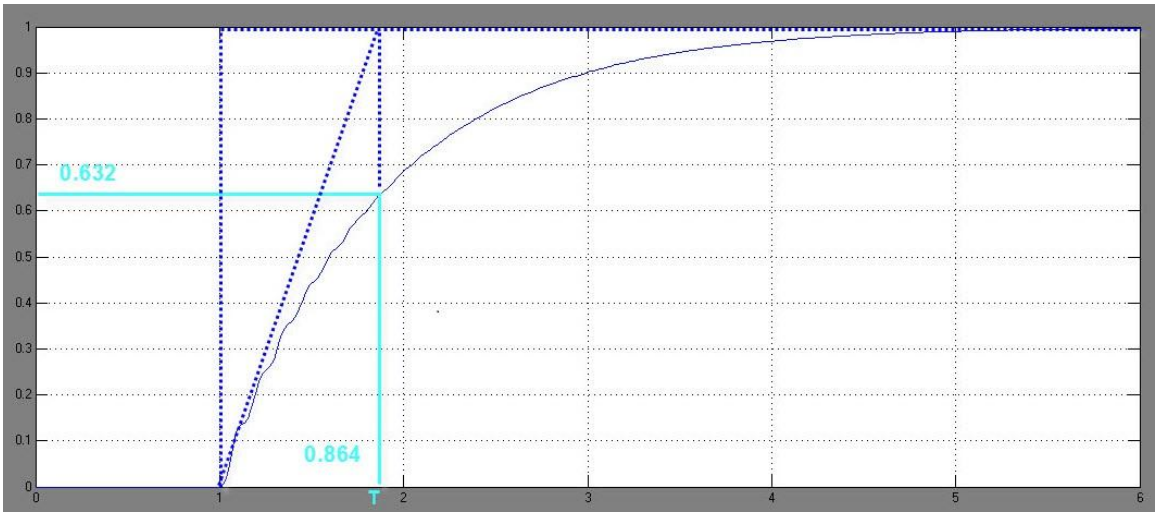

Figure 4.2 Step Response of the Vehicle Model (velocity vs. time in seconds)

For a typical first order delay, the transfer function basically has two parameters, a time constant τ and a close loop gain K and can be represented as [24]

$$H(s) = \frac{Y(s)}{U(s)} = \frac{K}{\tau s + 1} \tag{4.23}$$

or rewritten as input-output form as

$$Y(s) = \frac{K}{\tau s + 1} \cdot U(s) \tag{4.24}$$

Let $U(s)$ be a step input, which is $\frac{1}{s}$ in Laplace form, then $Y(s)$ can be represented as

$$Y(s) = \frac{K}{\tau s + 1} \cdot \frac{1}{s} = K\left(\frac{1}{s} - \frac{\tau}{\tau s + 1}\right) \tag{4.25}$$

Performing Inverse Laplace to the two sides of Equation 4.25, we obtain

$$y(t) = K\left(1 - e^{-\frac{t}{\tau}}\right) \tag{4.26}$$

Let t = τ and K = 1, from Equation 4.26,

$$y(\tau) = 1 - e^{-1} \approx 0.632 = 63.2\% \tag{4.27}$$

It can be clearly recognized that a first order delay is characterized in the step response and by measuring the corresponding time at magnitude of 63.2% of the step response [25]. From Equation 4.27, the time constant of the first order delay can be estimated, which is equal to 0.864s. Therefore a component of the dynamic system can be written as a first order delay with time constant $\tau_1 = 0.864s$, shown as follows:

$$y = \frac{1}{(\tau_1 s + 1)(\tau_2 s + 1)} u \tag{4.28}$$

where $\tau_1 = 0.864$ and τ_2 unknown.

Observing the step response, it's not difficult to notice that there are small waves around the beginning part of the response, which are caused by the other pole with a much smaller time constant, because when looking on a larger time scale, the influence of the pole with smaller time constant is limited and even hardly noticeable.

Using the Matlab System Identification toolbox, the other time constant τ_2 is estimated to be 0.002, exactly as what has been predicted, a much smaller time constant than that of the first order component. Since the pole corresponding to time constant τ_2 is much farther away from the vertical axis in a complex plane than that corresponding to time constant τ_1 (more than 10 times farther way), its influence to the whole system can be neglected when looking on a large scale in time.

4.3.1. Desired Headway Distance Based on Velocity of The Preceding Vehicle

As described in Section 4.1.1, the implementation of desired headway distance based on the velocity of the preceding vehicle is more straight-forward. In this section, two conditions are derived from what has been discussed above for this type of implementation, as shown in Figure 4.3.

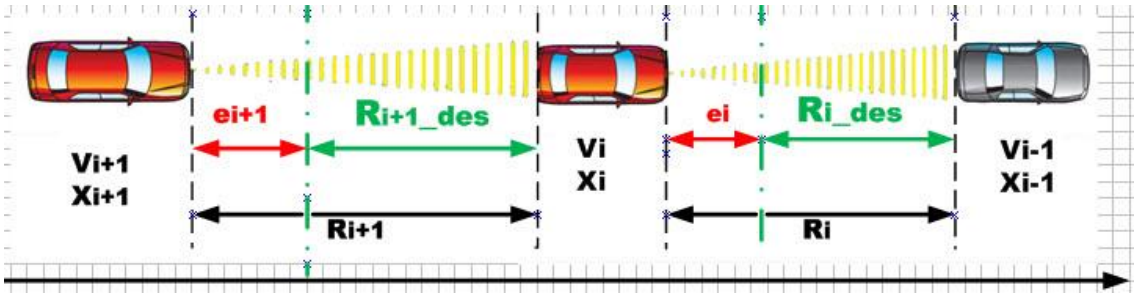

Figure 4.3 Vehicle Platoon

Theorem 4.1: For a string of vehicles to be string stable when the desired headway distance is based on velocity of the preceding vehicle, the following inequalities have to be met

$$\begin{cases} \left(2k_p\tau + k_p^2h^2 - 2k_d - 1\right)(\tau^2 - k_d^2h^2) \le 0 \\ \tau^2 - k_d^2h^2 \neq 0 \end{cases}$$

or

$$\begin{cases} 2k_p\tau + k_p^2h^2 - 2k_d - 1 \le 0 \\ \tau^2 - k_d^2h^2 = 0 \end{cases}$$

Proof: From analysis before, for the *i*-th vehicle in the platoon, Equation 4.22 can be simplified into the following equation:

$$\dot{x}_i = \frac{1}{\tau} e^{-\frac{t}{\tau}} \cdot \dot{x}_{i\_des}$$

or

$$sx_i(s) = \frac{1}{\tau s + 1} \cdot sx_{i_{des}}(s) \tag{4.29}$$

where τ is the dominant time constant, $\dot{x}_{i\_des}$ is the desired vehicle speed as system input and the output $\dot{x}_i$ is the actual vehicle speed.

Rewriting Equation 4.29 as

$$\tau\ddot{x}_i + \dot{x}_i = k_p \cdot \varepsilon_i + k_d \cdot \dot{\varepsilon}_i \tag{4.30}$$

where ε_i is the spacing error of the i-the vehicle, k_p and k_d are the parameters of the PD controller for headway control, and $(k_p \cdot \varepsilon_i + k_d \cdot \dot{\varepsilon}_i)$ serves as control input [26].

From Equation 4.30, change the index of each term from i to i-1,

$$\tau \ddot{x}_{i-1} + \dot{x}_{i-1} = k_p \cdot \varepsilon_{i-1} + k_d \cdot \dot{\varepsilon}_{i-1} \tag{4.31}$$

From the definition of spacing error, refer to Figure 4.3,

$$\varepsilon_i = R_i - h \cdot v_{i-1} = R_i - h \cdot \dot{x}_{i-1} \tag{4.32}$$

Differentiating the two sides of Equation 4.32 yields

$$\dot{\varepsilon}_i = \dot{R}_i - h \cdot \ddot{x}_{i-1} \tag{4.33}$$

Rewriting Equation 4.32 and Equation 4.33, one obtains

$$\dot{x}_{i-1} = \frac{1}{h}(R_i - \varepsilon_i)$$
$$\ddot{x}_{i-1} = \frac{1}{h}\left(\dot{R}_i - \dot{\varepsilon}_i\right) \tag{4.34}$$

Substituting $\dot{x}_{i-1}$ and $\ddot{x}_{i-1}$ in Equation 4.31 for Equation 4.34 yields

$$\frac{\tau}{h}\left(\dot{R}_i - \dot{\varepsilon}_i\right) + \frac{1}{h}(R_i - \varepsilon_i) = k_p \cdot \varepsilon_{i-1} + k_d \cdot \dot{\varepsilon}_{i-1}$$

Taking Laplace Transform to the equation, we obtain

$$R_i(s) = \varepsilon_i(s) + \frac{k_p h + k_d h s}{\tau s + 1} \cdot \varepsilon_{i-1}(s) \tag{4.35}$$

Changing the index of each term in Equation 4.32 from *i* to *i*-1 yield

$$\varepsilon_{i-1} = R_{i-1} - h \cdot \dot{x}_{i-2} \tag{4.36}$$

Subtracting the two sides of Equation 4.32 from the two sides of Equation 4.36, one obtains

$$\begin{aligned}\varepsilon_{i-1} - \varepsilon_i &= R_{i-1} - R_i + h(\dot{x}_{i-1} - \dot{x}_{i-2}) \\ &= R_{i-1} - R_i + h\dot{R}_{i-1}\end{aligned} \tag{4.37}$$

Performing Laplace transform to Equation 4.37, we obtain

$$\varepsilon_{i-1}(s) - \varepsilon_i(s) = R_{i-1}(s) - R_i(s) + hsR_{i-1}(s) \tag{4.38}$$

Substituting $R_i(s)$ in Equation 4.38 for Equation 4.35 and rearranging the two sides yields

$$R_{i-1}(s) = \frac{1}{1-hs}\left(1 + \frac{k_p h + k_d hs}{\tau s + 1}\right)\varepsilon_{i-1}(s) \tag{4.39}$$

Changing the index of Equation 4.39 from i-1 to i, we obtain

$$R_i(s) = \frac{1}{1-hs}\left(1 + \frac{k_p h + k_d hs}{\tau s + 1}\right)\varepsilon_i(s) \tag{4.40}$$

Substituting $R_i(s)$ and $R_{i-1}(s)$ in Equation 4.38 for Equation 4.39 and Equation 4.40, the error transfer function could be derived as

$$H(s) = \frac{\varepsilon_i(s)}{\varepsilon_{i-1}(s)} = \frac{-k_d hs^2 + (k_d - k_p h)s + k_p}{\tau s^2 + (k_d + 1)s + k_p} \tag{4.41}$$

From Section 4.2, for a platoon of vehicle to maintain string stability, the norm of error transfer function has to be less or equal to 1 for any angular frequency ω, therefore,

$$|H(j\omega)| = \left|\frac{\varepsilon_i(j\omega)}{\varepsilon_{i-1}(j\omega)}\right| \leq 1$$

Then the following equation can be derived from the above condition,

$$\omega^2 \geq \frac{2k_p\tau + k_p^2 h^2 - 2k_d - 1}{\tau^2 - k_d^2 h^2} \tag{4.42}$$

The above inequality has to hold for all ω to ensure string stability, which requires that

$$\frac{2k_p\tau + k_p^2h^2 - 2k_d - 1}{\tau^2 - k_d^2h^2} \leq 0$$

then the following conditions can be derived,

$$\begin{cases} \left(2k_p\tau + k_p^2h^2 - 2k_d - 1\right)(\tau^2 - k_d^2h^2) \leq 0 \\ \tau^2 - k_d^2h^2 \neq 0 \end{cases} \tag{4.43}$$

or

$$\begin{cases} 2k_p\tau + k_p^2h^2 - 2k_d - 1 \leq 0 \\ \tau^2 - k_d^2h^2 = 0 \end{cases} \tag{4.44}$$

4.3.2. Desired Headway Distance Based on Velocity of The Following Vehicle

As discussed in Section 4.1.2, a different definition of desired headway distance would lead to different conditions for string stability. In Section 4.3.1, conditions for the first case have been derived, while in this section, condition for the second case will be discussed.

Theorem 4.2: For a string of vehicles to be string stable when the desired headway distance is based on velocity of the preceding vehicle, the following inequalities have to be met

$$k_p^2h^2 + 2k_d + 1 - 2k_p(h - \tau) \geq 0$$

Proof: Equation 4.23 and Equation 4.24 still hold in this case. Different definition of desired headway distance leads to a different definition of headway spacing error of the *i*-th vehicle, which is shown as follows,

$$\varepsilon_i = R_i - h \cdot v_i = R_i - h \cdot \dot{x}_i \tag{4.45}$$

Differentiating the two sides of Equation 4.45 yields

$$\dot{\varepsilon}_i = \dot{R}_i - h \cdot \ddot{x}_i \tag{4.46}$$

Equation 4.45 and Equation 4.46 can be rewritten as follows:

$$\dot{x}_i = \frac{1}{h}(R_i - \varepsilon_i)$$
$$\ddot{x}_i = \frac{1}{h}\left(\dot{R}_i - \dot{\varepsilon}_i\right) \tag{4.47}$$

Substituting $\dot{x}_i$ and $\ddot{x}_i$ in Equation 4.24 for Equation 4.47, we obtain

$$\frac{\tau}{h}\left(\dot{R}_i - \dot{\varepsilon}_i\right) + \frac{1}{h}(R_i - \varepsilon_i) = k_p \cdot \varepsilon_i + k_d \cdot \dot{\varepsilon}_i \tag{4.48}$$

By rearranging the two sides of the Equation 4.48 and performing Laplace transform, one obtains

$$R_i(s) = \frac{hk_p + hk_d s + \tau s + 1}{\tau s + 1} \cdot \varepsilon_i(s) \tag{4.49}$$

Changing the index of Equation 4.46 and Equation 4.49 from i to i-1 yields

$$\dot{\varepsilon}_{i-1} = \dot{R}_{i-1} - h \cdot \ddot{x}_{i-1} \tag{4.50}$$
$$R_{i-1}(s) = \frac{hk_p + hk_d s + \tau s + 1}{\tau s + 1} \cdot \varepsilon_{i-1}(s) \tag{4.51}$$

Subtracting the two sides of Equation 4.46 from the two sides of Equation 4.50, we obtain

$$\varepsilon_{i-1}(s) - \varepsilon_i(s) = R_{i-1}(s) - (1 + hs)R_i(s) \tag{4.52}$$

Substituting $R_{i-1}(s)$ and $R_i(s)$ in Equation 4.52 for Equation 4.49 and Equation 4.51, the error transfer function could be derived as follows,

$$H(s) = \frac{\varepsilon_i(s)}{\varepsilon_{i-1}(s)} = \frac{k_p + k_d s}{(hk_d + \tau)s^2 + \left(hk_p + k_d + 1\right)s + k_p} \tag{4.53}$$

From Section 4.2, for a platoon of vehicle to maintain string stability, the norm of error transfer function has to be less or equal to 1 for any angular frequency ω, therefore

$$|H(j\omega)| = \left|\frac{\varepsilon_i(j\omega)}{\varepsilon_{i-1}(j\omega)}\right| \leq 1$$

The following equation can be derived from the above condition,

$$\left|\frac{k_p + k_d \cdot j\omega}{-(hk_d + \tau)\omega^2 + (hk_p + k_d + 1)j\omega + k_p}\right| \leq 1$$

$$\omega^2 \geq \frac{2k_p(\tau - h) - k_p^2 h^2 - 2k_d - 1}{(hk_d + \tau)^2}$$

$$\Rightarrow k_p^2 h^2 + 2k_d + 1 - 2k_p(h - \tau) \geq 0 \qquad (4.54)$$

Therefore if inequality (4.54) holds, string stability is ensured in this case.

4.4. Simulation Results

Simulation Case 1:

In the case described in Section 4.3.1, where the desired headway distance is defined based on velocity of the preceding vehicle, we use the following set of parameters that violates condition Equation 4.37 with $\tau = 0.864$,

$$k_p = 0.3, k_d = 9.6, h = 1.5$$

Figure 4.4 shows the results of a simulation which includes one lead vehicle and eight ACC equipped vehicles in a platoon, each of the vehicles has a on board headway controller with parameters above, Figure 4.5 shows the speed of each vehicles in the platoon.

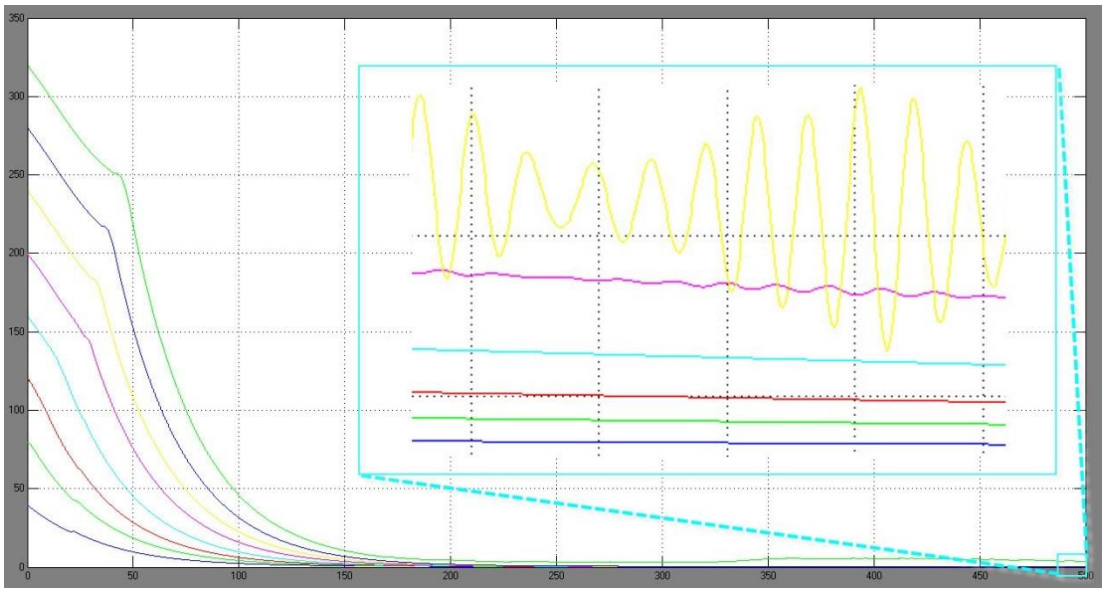

Figure 4.4 Amplification of Steady State Errors Along the Vehicle Platoon with Parameters That Violate Conditions for String Stability

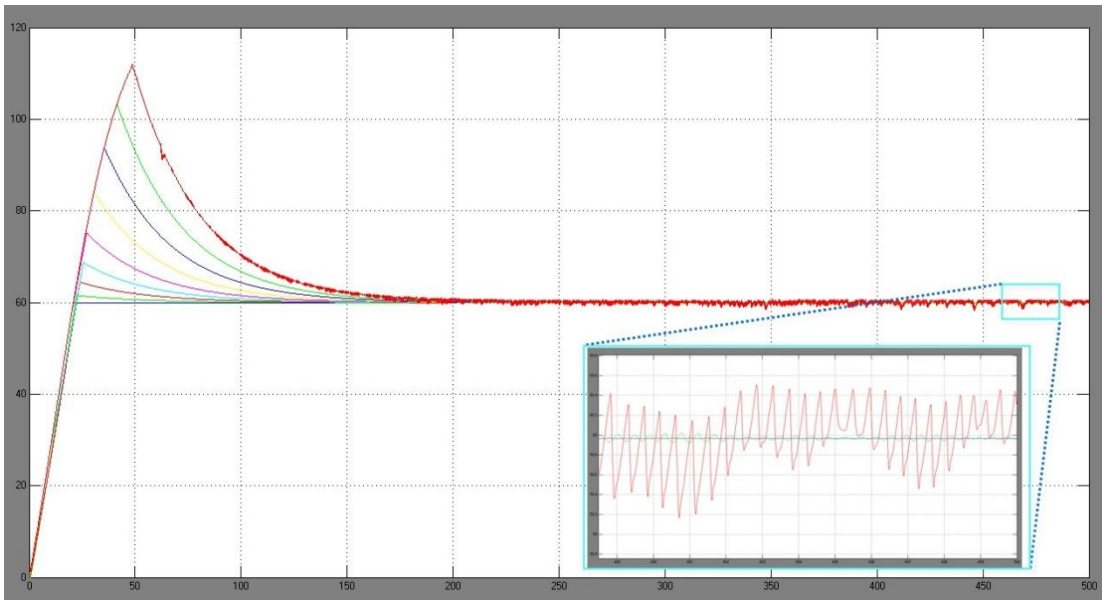

Figure 4.5 Speed Performance of Each Vehicle in the Platoon with Parameters That Violate Conditions for String Stability

Simulation Case 2:

Then we try to use another set of parameters that satisfies condition (4.38), which is

$$k_p = 0.1, k_d = 0.576, h = 1.5$$

Then there should be no amplification of steady state errors, shown in Figure 4.6, and Figure 4.7 shows the speed performance of each vehicle. This simulation shows results that is exactly as what has been theoretically predicted.

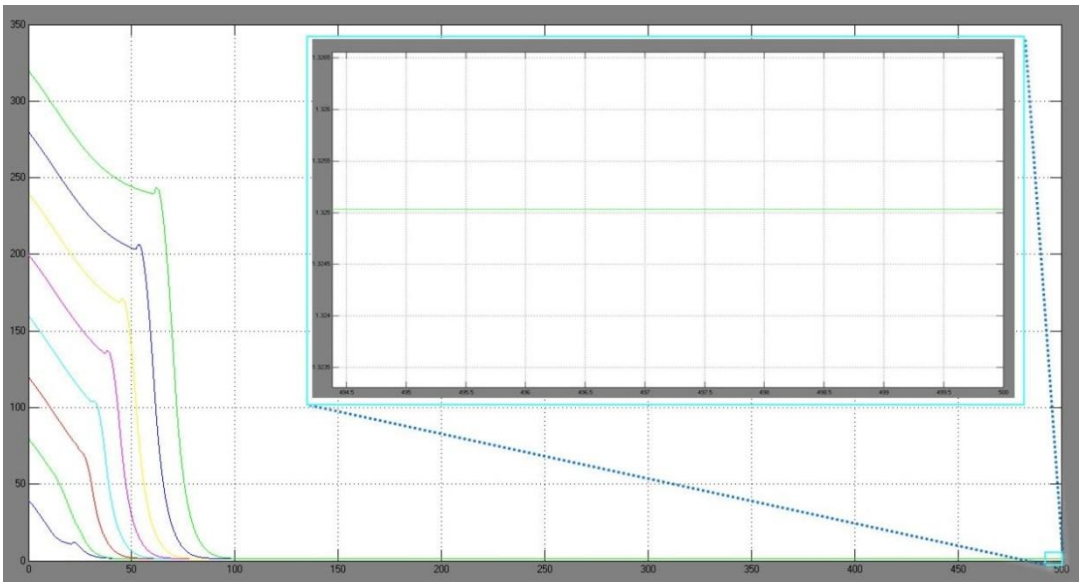

Figure 4.6 Amplification of Steady State Errors along the Vehicle Platoon with Parameters That Satisfy Conditions for String Stability

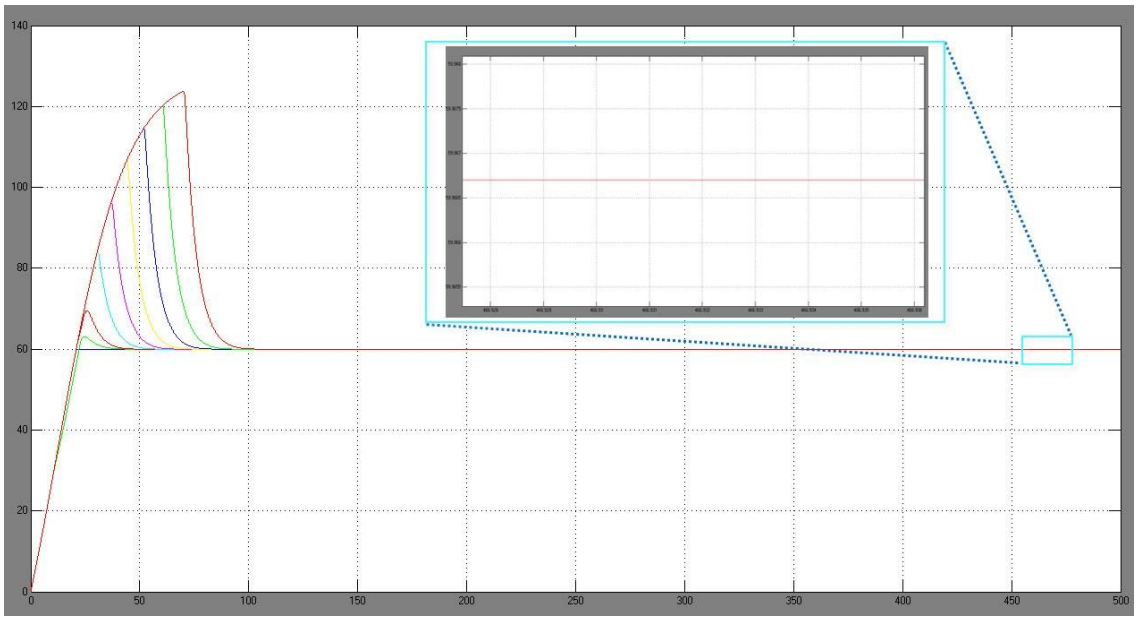

Figure 4.7 Speed Performance of Each Vehicle in the Platoon with Parameters That Satisfy Conditions for String Stability

4.5. Chapter Summary

In this chapter, the definition of string stability in a platoon of vehicles was discussed and mathematically described. General conditions for string stability have been derived. Conditions of string stability in steady state for two common implementations have also been discussed and mathematically derived.

5. CONCLUSION

In this thesis, we studied the algorithms of Adaptive Cruise Control (ACC) for common passenger vehicles and systematic pressures have been developed for implementations of such controller. In addition, string stability issues of a platoon of vehicles which are equipped with ACC controller have been discussed.

A longitudinal model of vehicle dynamic has been designed and verified on Matlab/Simulink environment. The vehicle dynamic equations depend on the longitudinal tire forces, aerodynamic drag forces, rolling resistance force and gravitational force. A systematic way to design ACC algorithms has been discussed in details. *R-Rdot* chart has been introduced to assist the design process. Constant deceleration of the following vehicle has been discussed to achieve a faster process to the equilibrium point, i.e. the desired headway distance to the preceding vehicle. Two constant deceleration levels have been chosen to be the upper limit and lower limit for the switching zone on an *R-Rdot* chart, according to the maximum deceleration level which human beings normally feel comfortable with. Simulations have shown a faster elapsed time than conventional design of ACC system, and maintained driving safety at the same time.

The string stability issues in situations where when many vehicles with ACC controller forming a vehicle platoon have been investigated. A generation of string stability of interconnected vehicles has been addressed and mathematically described. According to different definitions of desired headway distance, headway distance based on velocity of the preceding vehicle and based on that of the following vehicle, different conditions have been derived corresponding to each situation, respectively.

Corresponding to each case, simulations have been conducted and the results are quite satisfactory indeed.

Possible future works involve (1) using advanced control algorithms instead of PID to improve performance, (2) using more aggressive switching logic to further shorten elapsed time during transient process, and (3) taking sensor noise influence into consideration.

LIST OF REFERENCES

LIST OF REFERENCES

[1] P. Fancher, *et al.*, “Intelligent cruise control field operational test,” *DOT HS*, vol. 808, p. 849, 1998.

[2] J. Woll, "Radar-based adaptive cruise control for truck applications," *International Truck & Bus Meeting & Exposition*, Nov. 1997.

[3] D. Swaroop, J.K. Hedrick, "String stability of interconnected systems," *IEEE Trans. Automatic Control.*, vol. 41, no. 3, pp. 349-357, Mar. 1996.

[4] J.K. Hedrick, D. McMahon, D. Swaroop, "Vehicle modeling and control for automated highway systems," PATH Report, Institute of Transportation Studies, UC Berkeley, UCB-ITS-PRP-93-24, Nov. 1993.

[5] J.K. Hedrick, D. McMahon, V. Narendran, D. Swaroop, "Longitudinal vehicle controller design for IVHS systems," *American Control Conference*, pp. 3107-3112, 1991.

[6] D. Swaroop, *et al.*, “A Comparision of Spacing and Headway Control Laws for Automatically Controlled Vehicles,” *Vehicle System Dynamics*, vol. 23, pp. 597-625, 1994.

[7] Reichart, G., Haller, R., Naab, K., "Driver assistance: BMW solutions for the future of individual mobility," in *Proc. of ITS World Congress*, 1996.

[8] D. Swaroop and J. Hedrick, “String stability of interconnected systems,” *IEEE Transactions on Automatic Control*, vol. 41, pp. 349 - 357, 1996.

[9] R. Rajamani and C. Zhu, “Semi-autonomous adaptive cruise control systems,” *IEEE Transitions on Vehicular Technology*, vol. 51, pp. 1186 - 1192, 2002.

[10] “A Compilation of Motor Vehicle Crash Data from the Fatal Accident Reporting System and the General Estimates System,” *US Department of Transportation, National Highway Traffic Safety Administration,* p. 50, 1994.

[11] 余志生，汽车理论，第三版．北京：机械工业出版社，2005. (Zhisheng Yu, *Automobile Theory, Third Edition*, Beijing: China Machine Press, 2005).

[12] R. Rajamani, *Vehicle dynamics and control*, Springer, 2006.

[13] E. Hendricks and S. Sorenson, “Mean value modeling of spark ignition engines,” *International Congress & Exposition,* 1990.

[14] Mathworks, Gasoline Engine Block Online Help Documents. Available: http://www.mathworks.com/help/toolbox/physmod/drive/gasolineengine.html.

[15] D. Cho and J. Hedrick, “Automotive powertrain modeling for control,” *Journal of Dynamic Systems, Measurement, and Control,* vol. 111, p. 568, 1989.

[16] A. Tugcu, *et al.*, “Modeling and simulation of the powertrain dynamics of vehicles equipped with automatic transmission,” pp. 39-61, 1987.

[17] J. Runde, *Modeling and Control of an Automatic Transmission*, Massachusetts Institute of Technology, 1986.

[18] H. Pacejka, “The tyre as a vehicle component,” XXVI FISITA Congress, 1996.

[19] Mathworks, Simulink Tire Model Online Help Documents. Available: http://www.mathworks.com/help/toolbox/physmod/drive/tire.html

[20] P. Ioannou and C. Chien, “Autonomous intelligent cruise control,” *IEEE Transactions on Vehicular Technology,* vol. 42, pp. 657-672, 1993.

[21] P. Fancher and Z. Bareket, "Evaluating headway control using range versus range-rate relationships," *Vehicle System Dynamics*, vol. 23, no. 1, pp. 575-596, 1994.

[22] P. Fancher, *et al.*, “Intelligent cruise control: Performance studies based upon an operating prototype,” 1994, pp. 391-399.

[23] C. Desoer and M. Vidyasagar, *Feedback Systems: Input-Output Properties*, Society for Industrial and Applied Mathematics, 2009.

[24] 徐薇莉, 曹柱中, 田作华, 自动控制理论与设计, 第三版: 上海交通大学出版社, 1995. (W. Xu, Z. Cao, and Z. Tian, *Automotive Control Theory and Design, Third Edition*: Shanghai Jiaotong University Press, 1995.)

[25] K. Ogata, *Modern Control Engineering*, Prentice Hall, 2009.

[26] K. Astrom and T. Hagglund, *PID Controllers: Theory, Design, and Tuning, Second Edition*, International Society for Measurement and Control, 1995.